

**2017 Fall**

**“Calculation and Applications Phase Equilibria”**

# **Principles *of* Solidification**

**06.05.2017**

**Eun Soo Park**

**Office: 33-313**

**Telephone: 880-7221**

**Email: [espark@snu.ac.kr](mailto:espark@snu.ac.kr)**

**Office hours: by appointment**

# Chapter 6 Polyphase solidification

## 6.1. Evolution of a Gas during solidification

### (a) Gas-metal equilibria

A typical solubility diagram

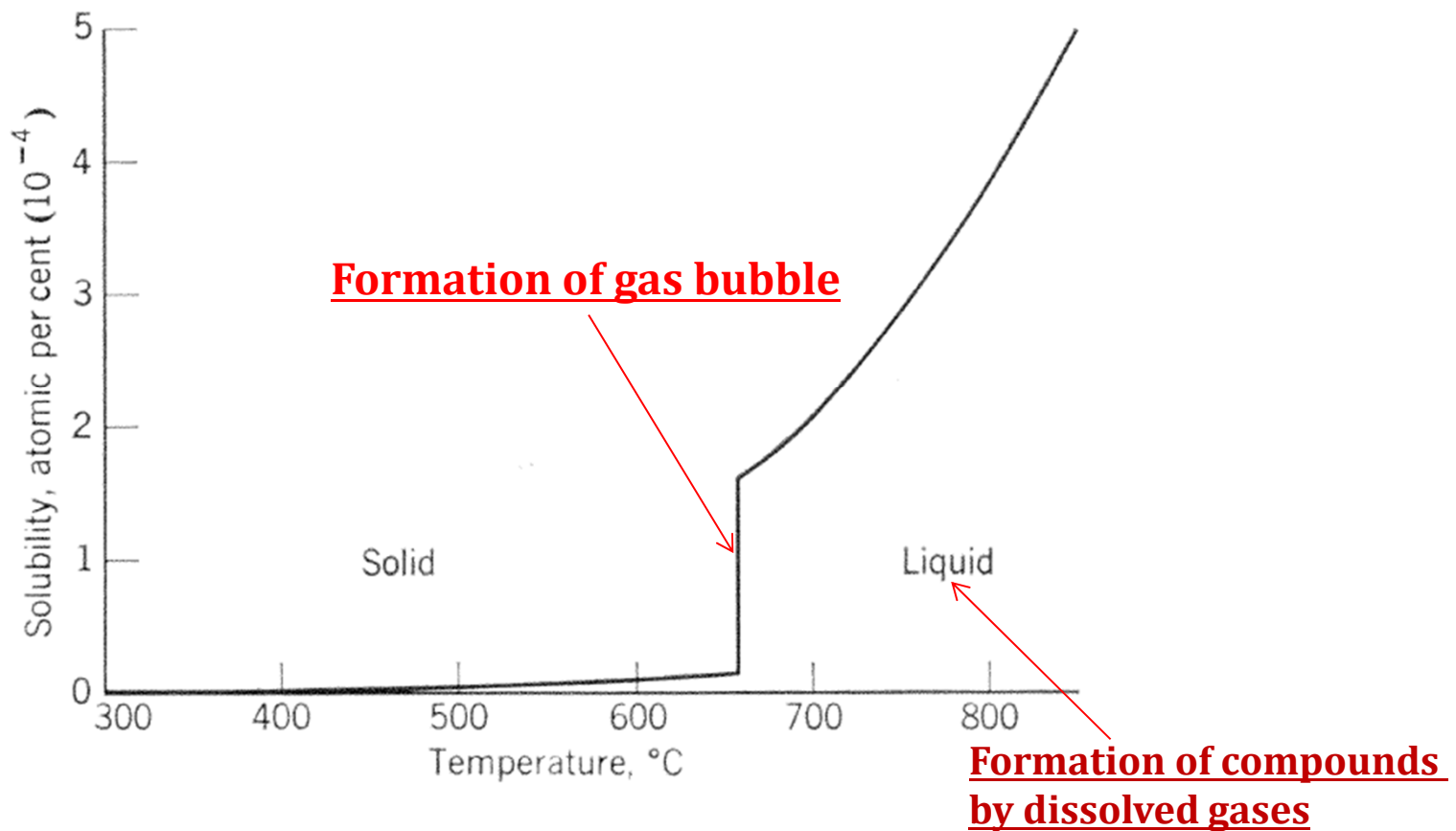


Fig. 6.2. Solubility of hydrogen in aluminum.

But , a solid-liquid interface should not be an effective nucleant for a bubble;

Equilibrium corresponds to  $\theta < 180^\circ$  ,

$$\sigma_{SL} = \sigma_{SG} + \sigma_{LG} \cos \theta$$

$$\cos \theta = \frac{\sigma_{SL} - \sigma_{SG}}{\sigma_{LG}}$$

$$\sigma_{SG} \gg \sigma_{SL} \ \& \ \sigma_{SG} > \sigma_{LG}$$

$$\therefore \cos \theta < -1$$

→ Surface E of the bubble is increased by contact with the solid-liquid interface.

However, gas bubbles are formed at solid-liquid interfaces.

This location is in part due to the fact that the gas concentration would be highest there during solidification; but it may also be due to the fact that any re-entrant in the interface, such as a cell wall, grain boundary, or interdendritic space, would have an even higher gas content because of lateral segregation, as shown in Fig. 6.5.

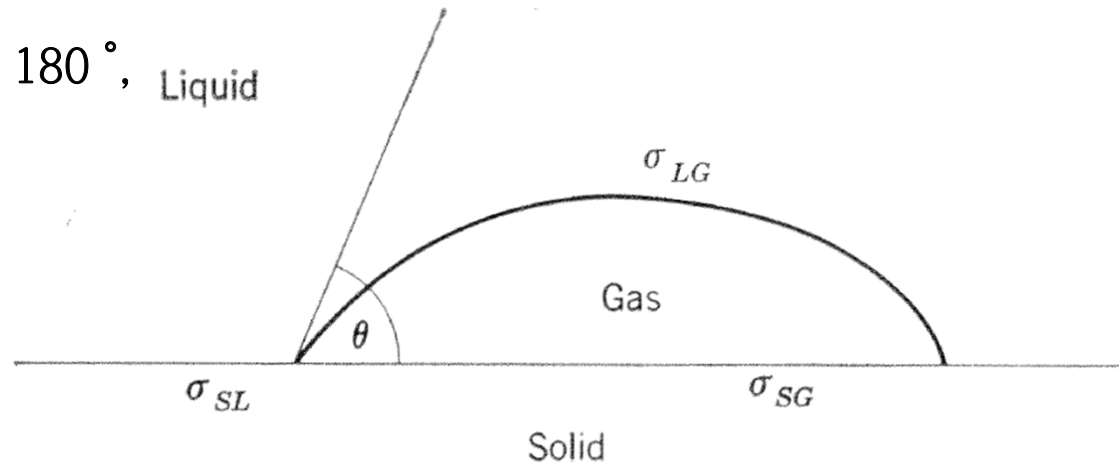
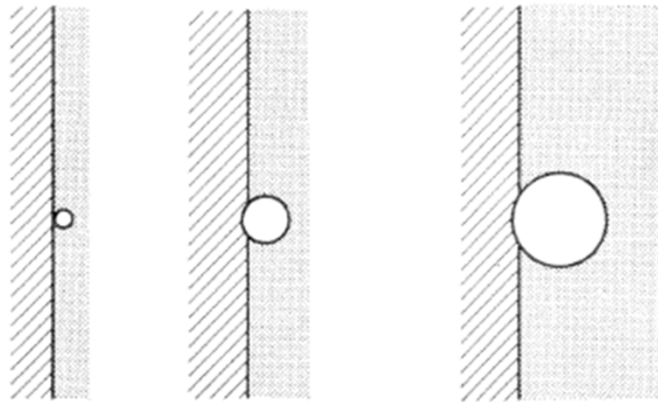


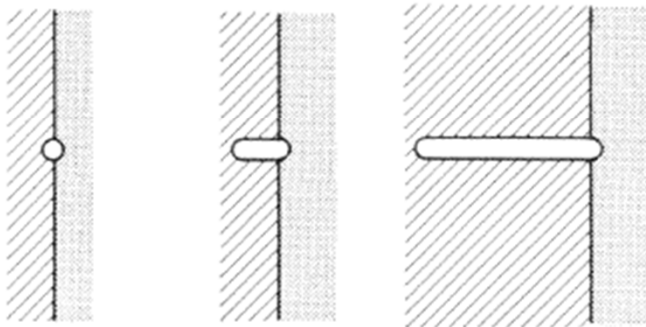
Fig. 6.4. Solid-liquid as nucleant for a gas bubble.



(a)

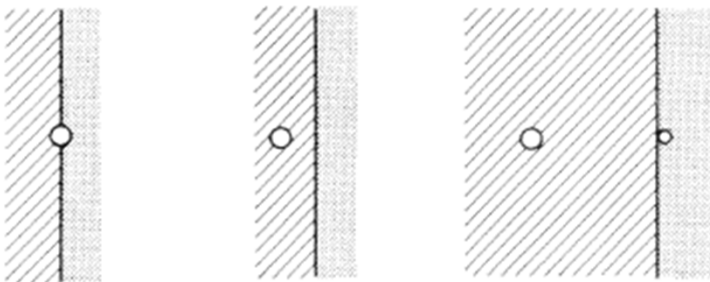
\* Growth rate of bubble  $>$  Advanced speed of interface  
 → increase of bubble diameter

**The diameter of the bubble is maintained in the longitudinal direction**



(b)

\* Growth rate of bubble  $\sim$  Advanced speed of interface  
 → Bubble growth progresses in the longitudinal direction while maintaining bubble diameter



(c)

\* Growth rate of bubble  $<$  Advanced speed of interface  
 → bubble are trapped in the solid.

Fig. 6.6. Effect of speed of growth of a bubble on its shape and size.  
 (a) Slow growth, (b) intermediate speed, (c) fast growth.

## 6.2 Eutectics: limited solubility, most fusible (가장 잘 녹는, Greek)

**\* Most of the discussion of eutectic solidification will be based on binary eutectic.**

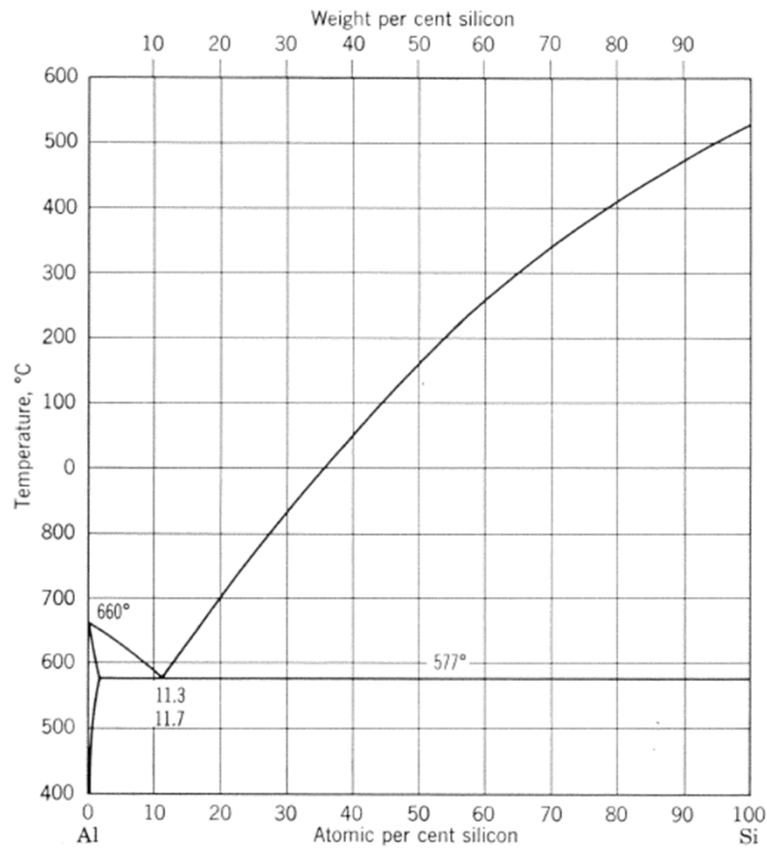


Fig. 6.9. Phase diagram for the Al-Si system

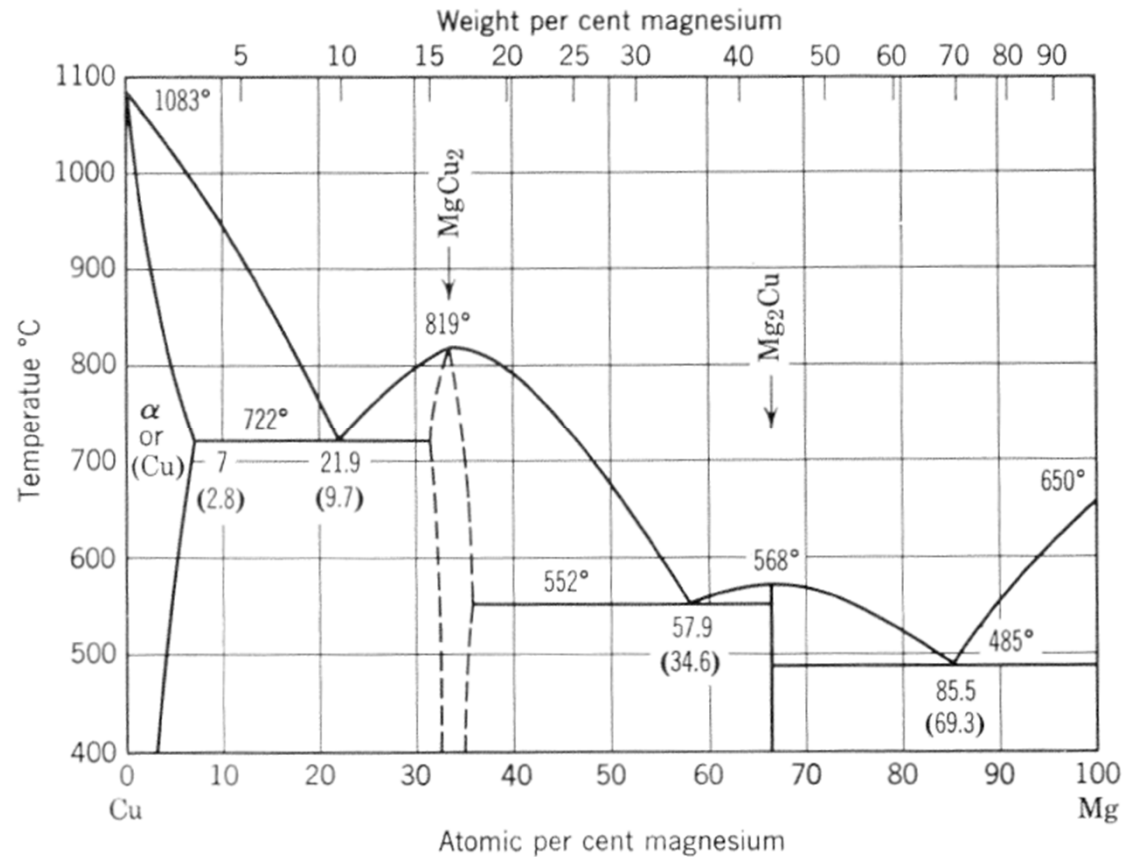
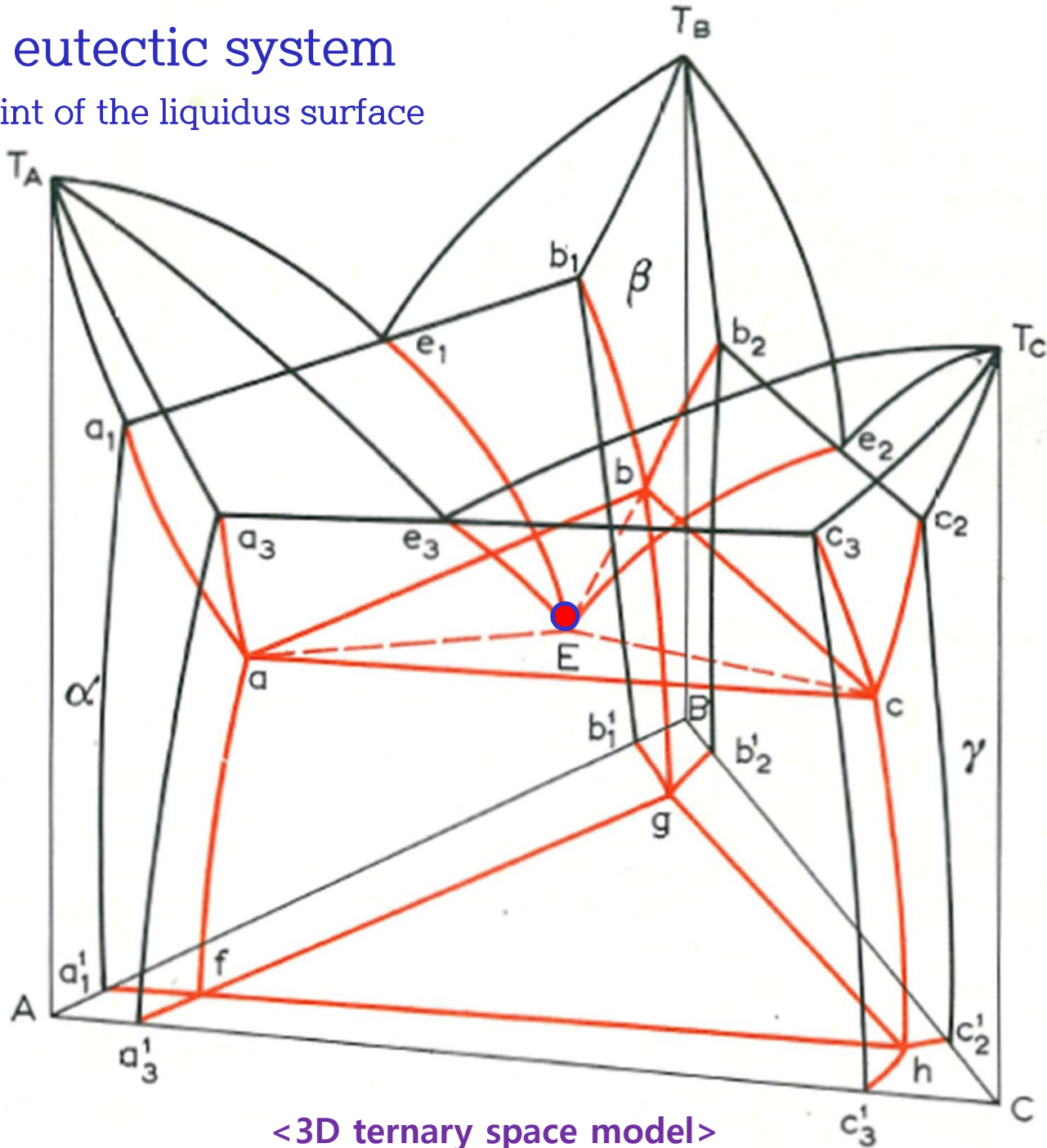


Fig. 6.10. Phase diagram for the Cu-Mg system

\* Ternary eutectic system

: Minimum point of the liquidus surface



<3D ternary space model>

\* Quaternary eutectic  $l \rightleftharpoons \alpha + \beta + \gamma + \delta$

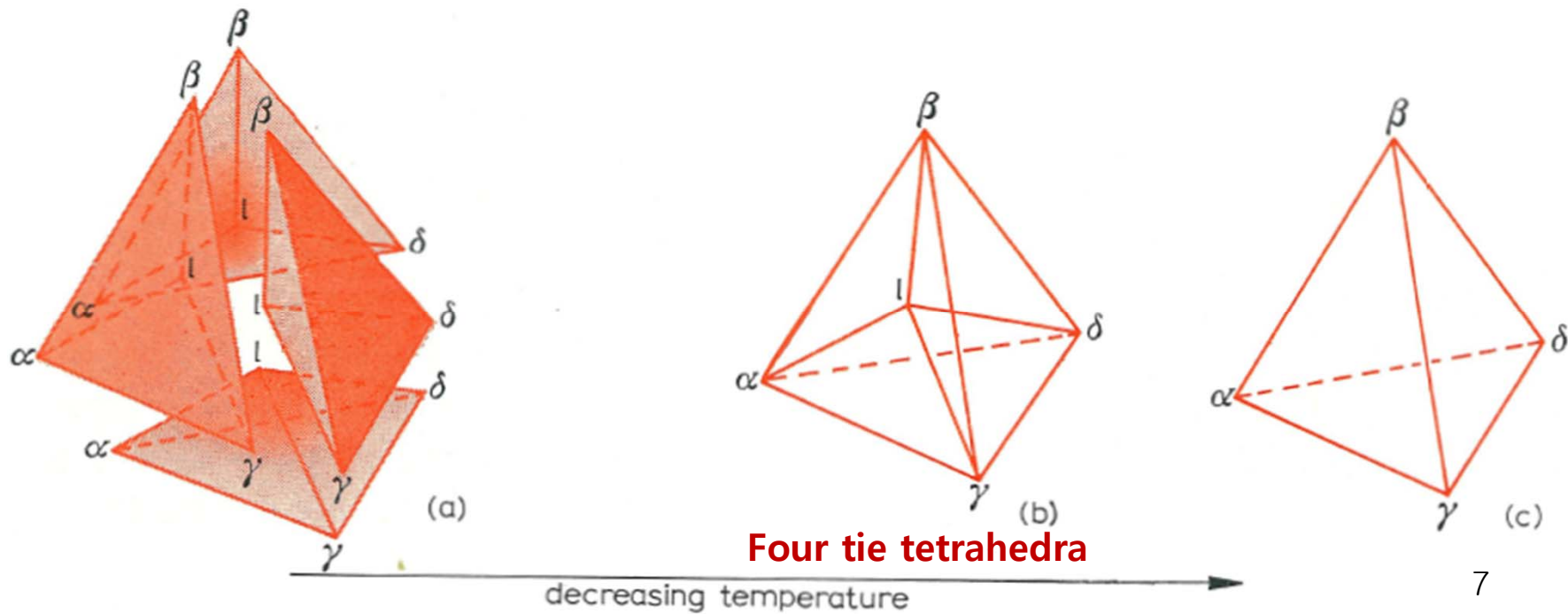
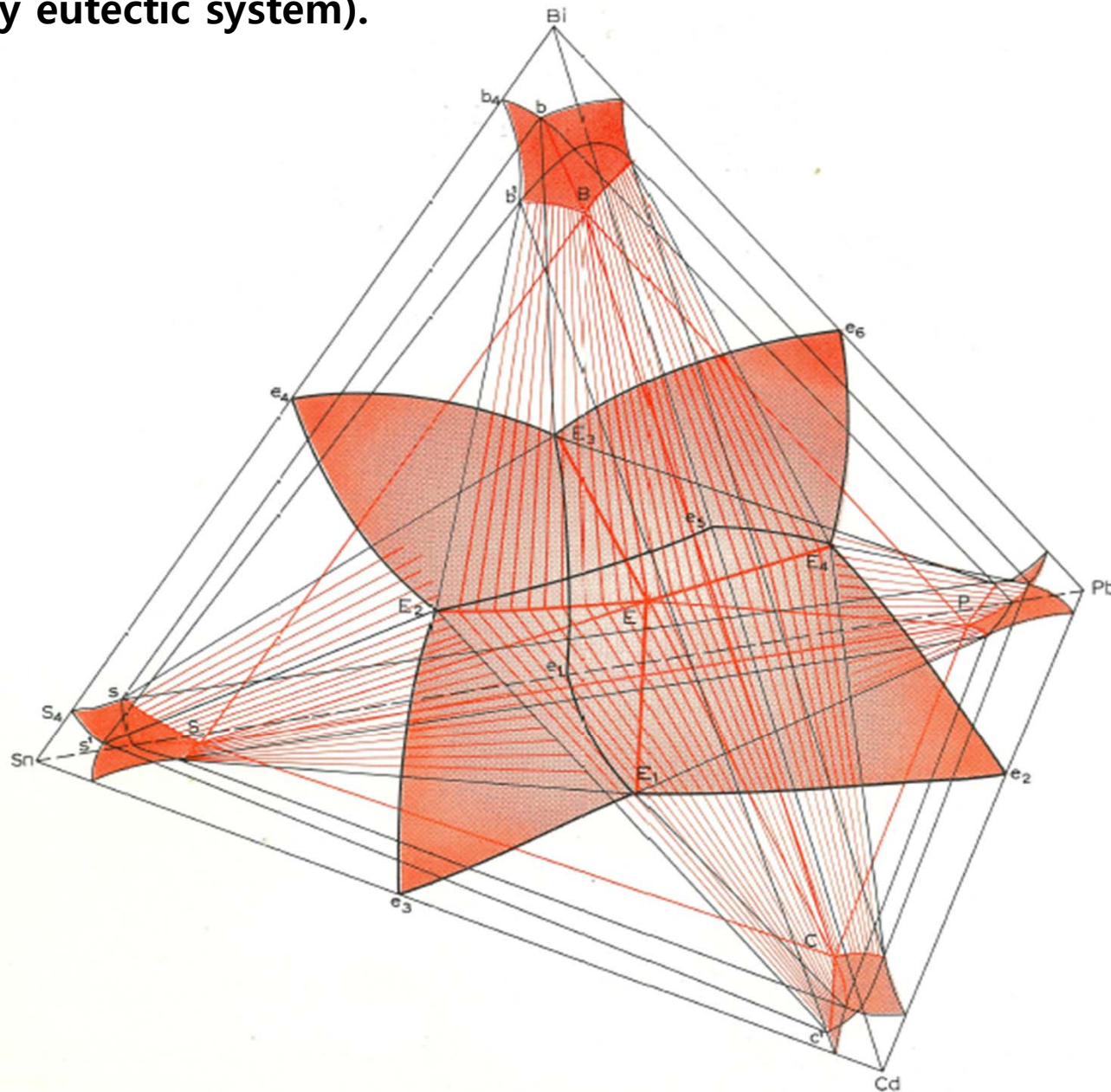


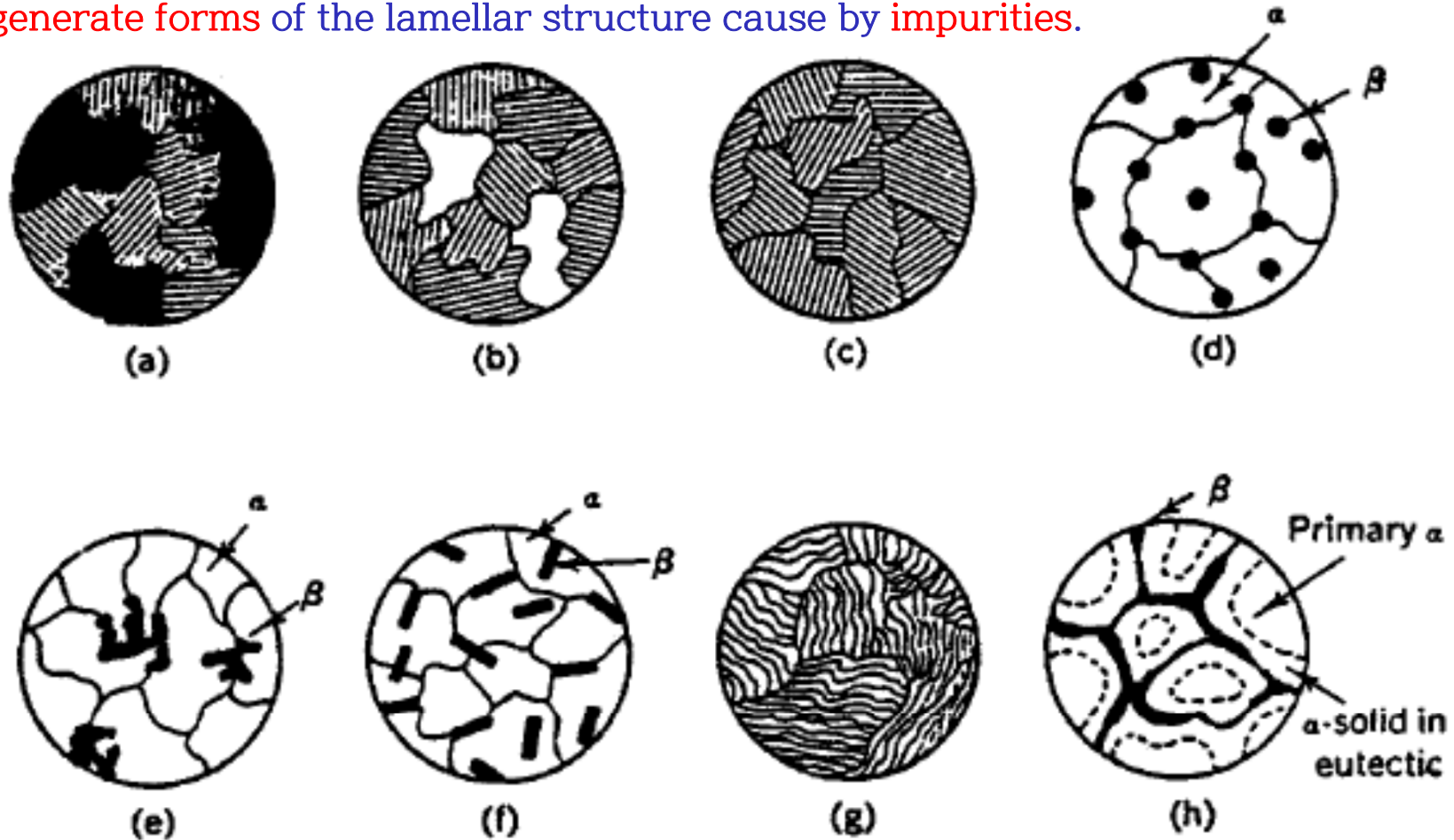
Fig. Sequence of tie-tetrahedron on cooling through the quaternary eutectic temperature

Polythermal projectin of a quaternary system involving five-phase equilibrium of the type  $l \rightleftharpoons \alpha + \beta + \gamma + \delta$  (schematic representation of the Bi-Cd-Pb-Sn quaternary eutectic system).



# 1) Microstructure of Eutectics

\* Many eutectics are lamellar with a very regular structure if the metals used are sufficiently “pure” and that many of the other structures that are observed are degenerate forms of the lamellar structure caused by impurities.



~~various~~

Fig. 14 Schematic representation possible in eutectic structures. (a), (b) and (c) are alloys shown in fig. 13; (d) nodular; (e) Chinese script; (f) acicular; (g) lamellar; and (h) divorced.

### 3) Solidification of lamellar eutectic

Two representative opinions:

- 1) Tammann : alternation of layers of the two phases
- 2) Vogel: two phase grew simultaneously → interlamellar interfaces were approximately normal to the mean solid-liquid interface

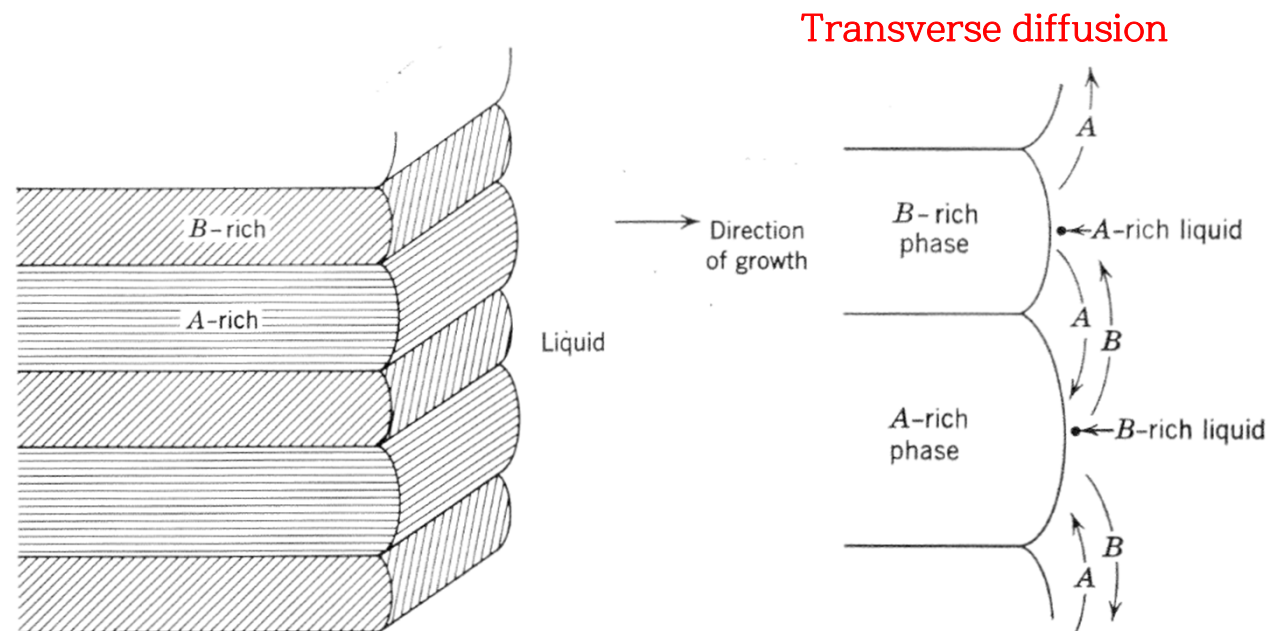
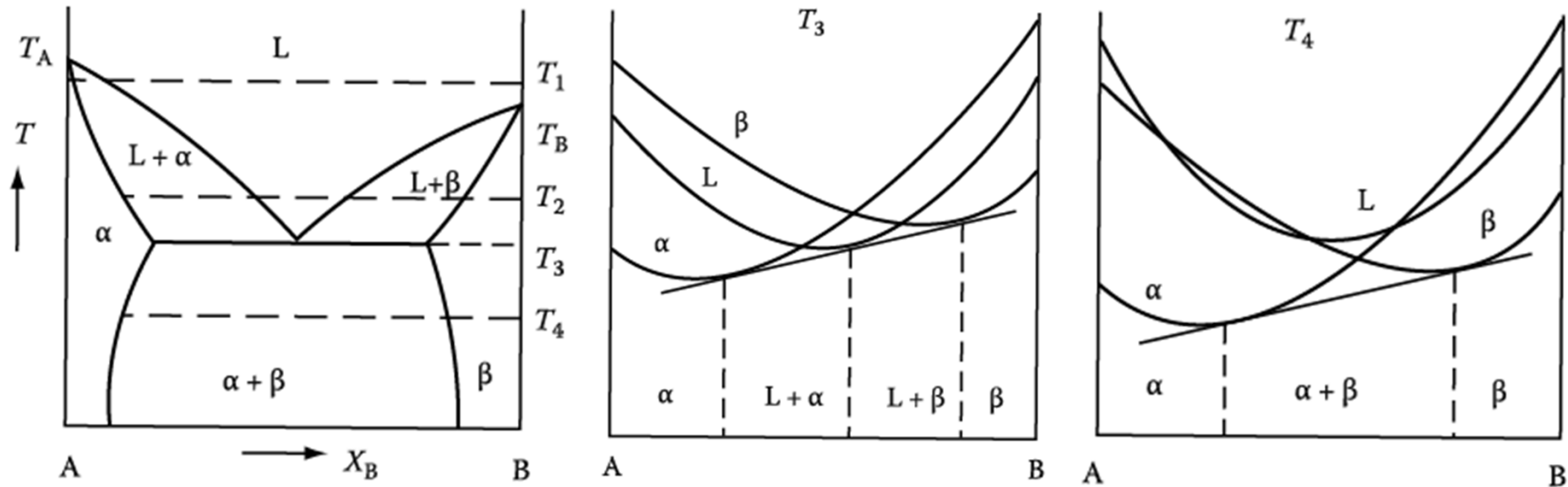


Fig. 6.14. Growth, mechanism, and diffusion paths for lamellar eutectic.

**Q: Thermodynamics and Kinetics of eutectic solidification ( $L \rightarrow \alpha + \beta$ ) ?**

This section will only be concerned with normal structures, and deal mainly with lamellar morphologies.

## 2. Eutectic Solidification (Thermodynamics)



Plot the diagram of Gibbs free energy vs. composition at  $T_3$  and  $T_4$ .

What is the driving force for the eutectic reaction ( $L \rightarrow \alpha + \beta$ ) at  $T_4$  at  $C_{\text{eut}}$ ?

What is the driving force for nucleation of  $\alpha$  and  $\beta$ ? “ $\Delta T$ ”

# Eutectic Solidification (Kinetics)

:  $\Delta T \rightarrow$  formation of interface + solute redistribution

If  $\alpha$  is nucleated from liquid and starts to grow, what would be the composition at the interface of  $\alpha/L$  determined?

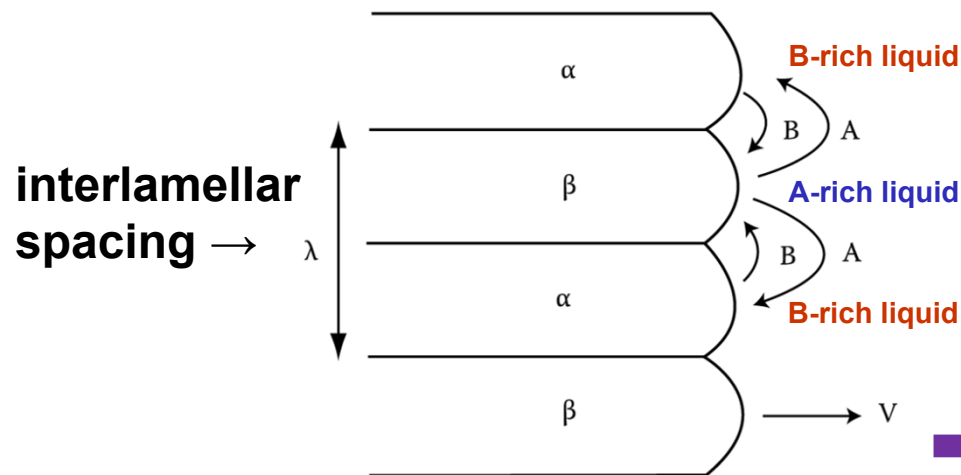
$\rightarrow$  rough interface (diffusion interface) & local equilibrium

How about at  $\beta/L$ ? Nature's choice? Lamellar structure

$$\rightarrow G = G_{\text{bulk}} + G_{\text{interface}} = G_0 + \gamma A$$

$$\sum A_i \gamma_i + \Delta G_S = \text{minimum}$$

Interface energy + Misfit strain energy



**Eutectic solidification**  
: diffusion controlled process

1)  $\lambda \downarrow \rightarrow$  eutectic growth rate  $\uparrow$

but 2)  $\lambda \downarrow \rightarrow \alpha/\beta$  interfacial E,  $\gamma_{\alpha\beta} \uparrow$   
 $\rightarrow$  lower limit of  $\lambda$

fastest growth rate at a certain  $\lambda$

What would be a role of the curvature at the tip?

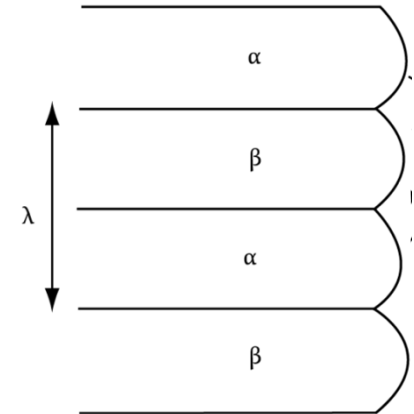
$\rightarrow$  Gibbs-Thomson Effect

# Eutectic Solidification (Kinetics)

:  $\Delta T \rightarrow$  a) formation of interface + b) solute redistribution

How many  $\alpha/\beta$  interfaces per unit length?

$\rightarrow 1/\lambda \times 2$



a) Formation of interface:  $\Delta G$

For an interlamellar spacing,  $\lambda$ , there is a total of  $(2/\lambda) \text{ m}^2$  of  $\alpha/\beta$  interface per  $\text{m}^3$  of eutectic.

$$\Delta G = \Delta\mu \cong \frac{L\Delta T}{T_m}$$

$$\rightarrow \Delta G = \Delta\mu = \frac{2\gamma}{\lambda} \times V_m$$

Driving force for nucleation = Total interfacial E of eutectic phase

For very large values of  $\lambda$ , interfacial E  $\sim 0$

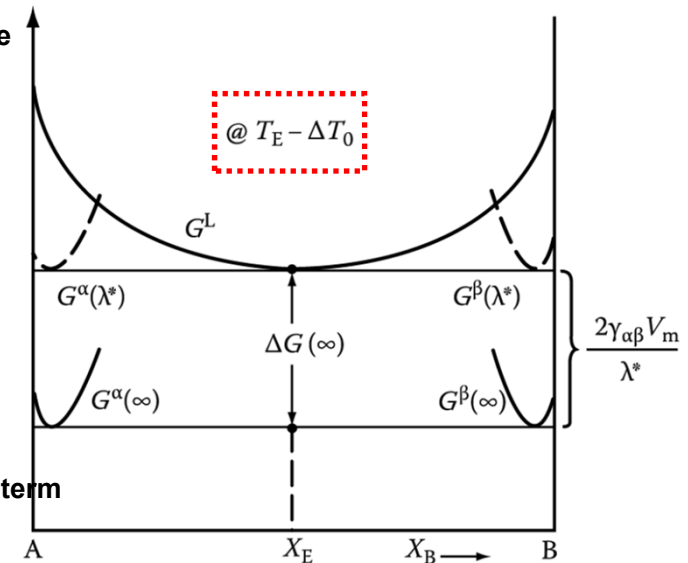
No interface (ideal case)

$$\lambda \rightarrow \infty, \quad \Delta G(\infty) = \Delta\mu = \frac{\Delta H \Delta T_0}{T_E}$$

With interface (real case)

$$\Delta G(\lambda) = ? = -\Delta G(\infty) + \frac{2\gamma V_m}{\lambda}$$

Solidification will take place if  $\Delta G$  is negative (-).



a) All  $\Delta T \rightarrow$  use for interface formation = min.  $\lambda$

What would be the minimum  $\lambda$ ?

Critical spacing,  $\lambda^* : \Delta G(\lambda^*) = 0$

최소 층상 간격

$$\Delta G(\infty) = \frac{2\gamma V_m}{\lambda^*}$$

$$\lambda^* = + \frac{2T_E \gamma V_m}{\Delta H \Delta T_0}$$

Gibbs-Thomson effect

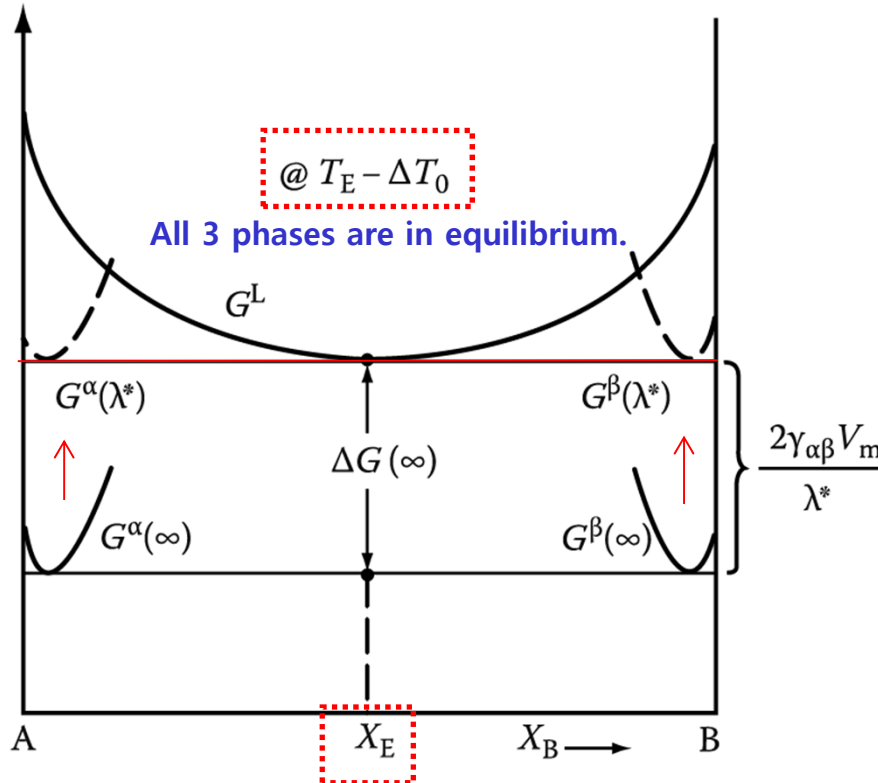
$$\lambda^* = -\frac{2T_E \gamma V_m}{\Delta H \Delta T_0} \rightarrow \text{identical to critical radius of dendrite tip in pure metal}$$

$$\text{cf) } r^* = \frac{2\gamma_{SL}}{\Delta G_V} = \left( \frac{2\gamma_{SL} T_m}{L_V} \right) \frac{1}{\Delta T}$$

$L_V$  : latent heat per unit volume  
 $L = \Delta H = H^L - H^S$

\* Growth Mechanism: Gibbs-Thomson effect in a  $\Delta G$ -composition diagram?

1) At  $\lambda = \lambda^* (< \infty)$ ,

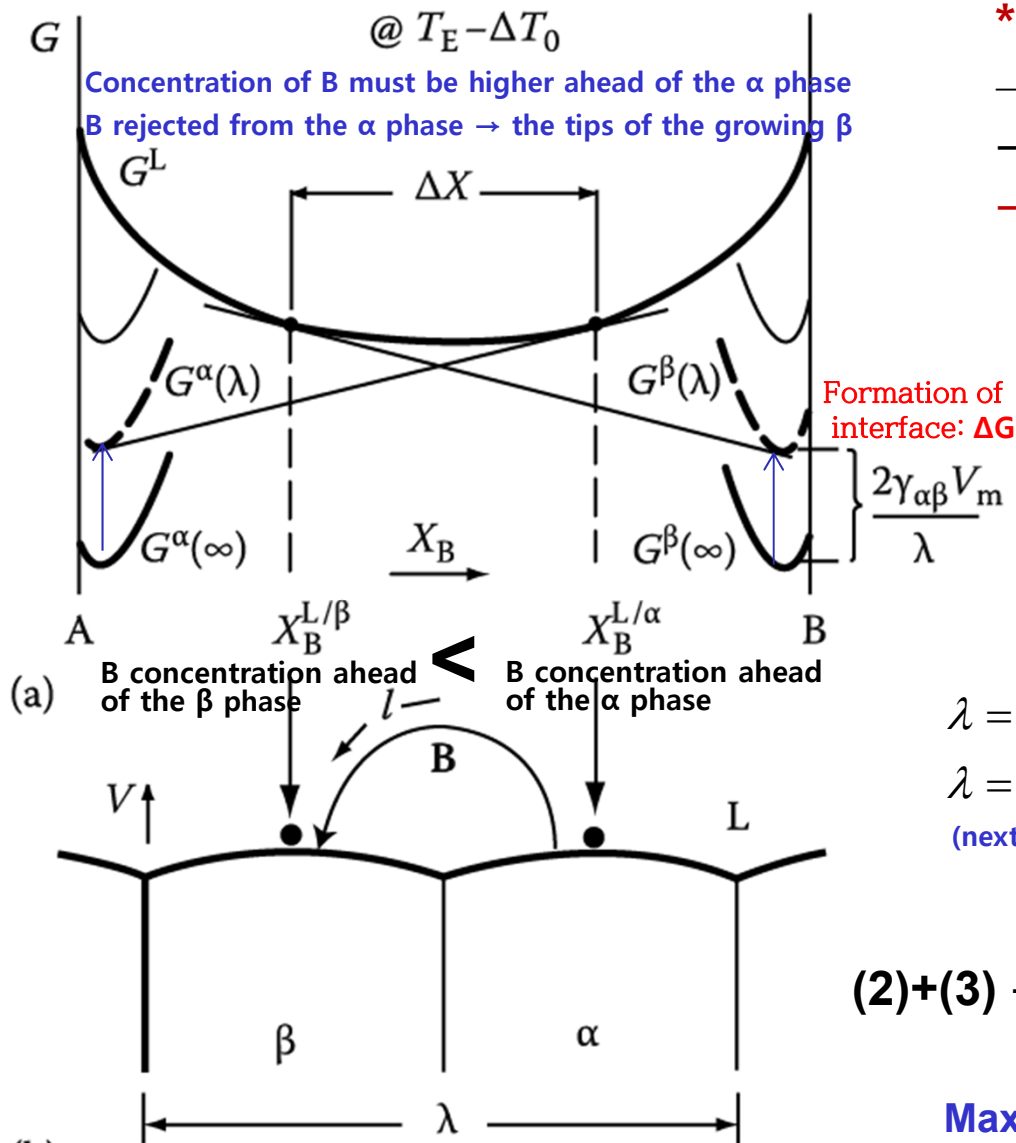


The cause of **G increase** is the curvature of the  $\alpha/L$  and  $\beta/L$  interfaces arising from the need to **balance the interfacial tensions at the  $\alpha/\beta/L$  triple point**, therefore the increase will be different for the two phases, but for simple cases it can be shown to be

$$\frac{2\gamma_{\alpha\beta}V_m}{\lambda} \text{ for both.}$$

1) If  $\lambda = \lambda^*$ , growth rate will be ***infinitely slow*** because the liquid in contact with both phases has the same composition,  $X_E$  in Figure 4.32.

2) At  $\lambda = (\infty >) \lambda (> \lambda^*)$ , If  $\infty > \lambda > \lambda^*$ ,  $G_\alpha$  and  $G_\beta$  are correspondingly reduced because less free energy is locked in the interfaces.  $\rightarrow X_B^{L/\alpha} > X_B^{L/\beta}$



\* Eutectic growth rate,  $v$

$\rightarrow$  if  $\alpha/L$  and  $\beta/L$  interfaces are highly mobile  
 $\rightarrow$  proportional to flux of solute through liquid

$\rightarrow$  **diffusion controlled process**

$$v \propto D \frac{dC}{dl} \propto (X_B^{L/\alpha} - X_B^{L/\beta})$$

$$\propto 1/\text{effective diffusion distance.. } 1/\lambda$$

$$v = k_1 D \frac{\Delta X}{\lambda} \quad (1)$$

$$\lambda = \lambda^*, \Delta X = 0$$

$$\lambda = \infty, \Delta X = \Delta X_0$$

(next page)

$$\Delta X = \Delta X_0 \left(1 - \frac{\lambda^*}{\lambda}\right) \quad (2)$$

$$\Delta X_0 \propto \Delta T_0 \quad (3)$$

$$(2)+(3) \rightarrow (1) \quad v = k_2 D \frac{\Delta T_0}{\lambda} \left(1 - \frac{\lambda^*}{\lambda}\right)$$

Maximum growth rate at a fixed  $\Delta T_0 \rightarrow \lambda = 2\lambda^*$

Fig. 4.33 (a) Molar free energy diagram at  $(T_E - \Delta T_0)$  for the case  $\lambda^* < \lambda < \infty$ , showing the composition difference available to drive diffusion through the liquid ( $\Delta X$ ). (b) Model used to calculate the growth rate. 16

$\Delta X$  will it self depend on  $\lambda$ .  $\sim$  maximum value,  $\Delta X_0$

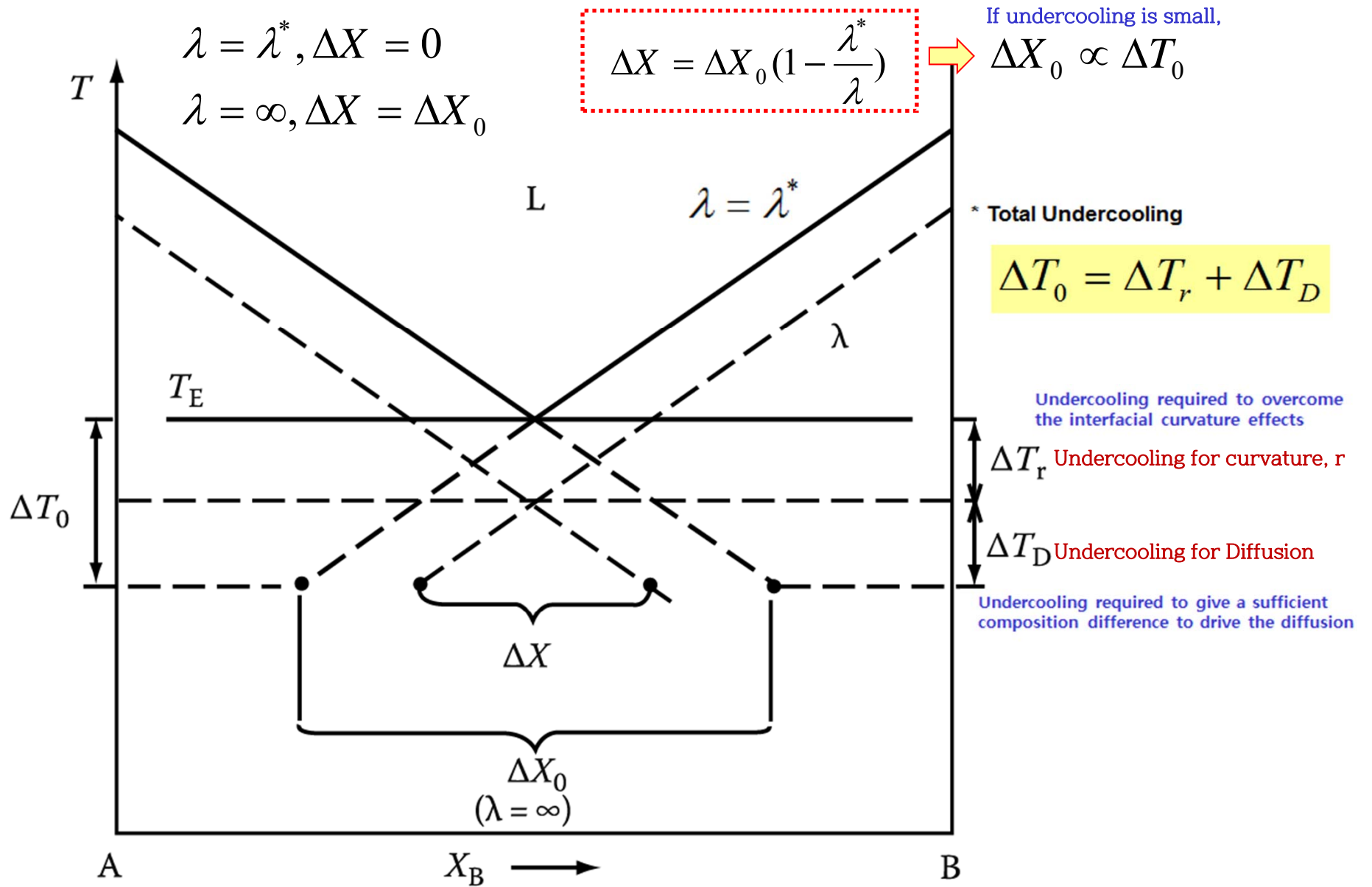
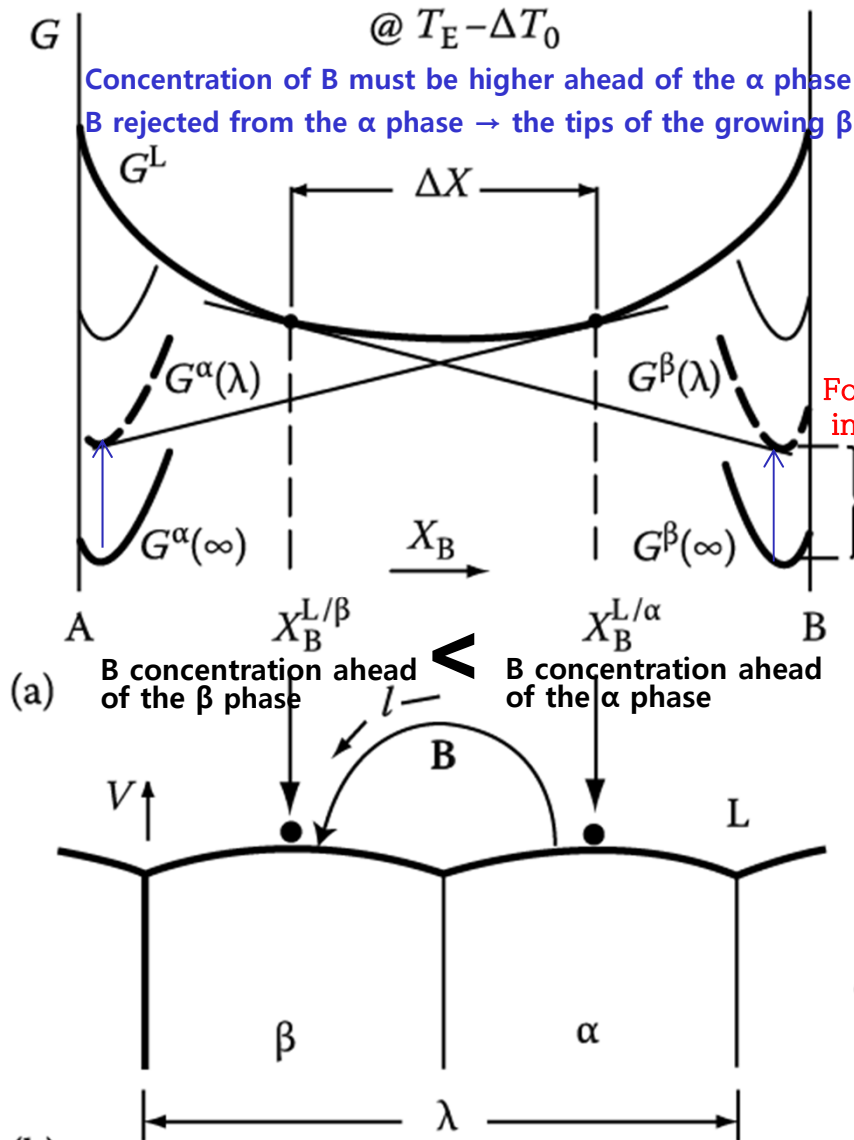


Fig. 4.34 Eutectic phase diagram showing the relationship between  $\Delta X$  and  $\Delta X_0$  (exaggerated for clarity)

2) At  $\lambda = (\infty >) \lambda (> \lambda^*)$ ,

If  $\infty > \lambda > \lambda^*$ ,  $G_\alpha$  and  $G_\beta$  are correspondingly reduced because less free energy is locked in the interfaces.  $\rightarrow X_B^{L/\alpha} > X_B^{L/\beta}$



\* Eutectic growth rate,  $v$

$\rightarrow$  if  $\alpha/L$  and  $\beta/L$  interfaces are highly mobile

$\rightarrow$  proportional to flux of solute through liquid

$\rightarrow$  diffusion controlled process

$$v \propto D \frac{dC}{dl} \propto (X_B^{L/\alpha} - X_B^{L/\beta})$$

$$\propto 1/\text{effective diffusion distance.. } 1/\lambda$$

$$v = k_1 D \frac{\Delta X}{\lambda} \quad (1)$$

$$\lambda = \lambda^*, \Delta X = 0$$

$$\lambda = \infty, \Delta X = \Delta X_0$$

(next page)

$$\Delta X = \Delta X_0 \left(1 - \frac{\lambda^*}{\lambda}\right) \quad (2)$$

$$\Delta X_0 \propto \Delta T_0 \quad (3)$$

$$(2)+(3) \rightarrow (1) \quad v = k_2 D \frac{\Delta T_0}{\lambda} \left(1 - \frac{\lambda^*}{\lambda}\right)$$

Maximum growth rate at a fixed  $\Delta T_0 \rightarrow \lambda = 2\lambda^*$

Fig. 4.33 (a) Molar free energy diagram at  $(T_E - \Delta T_0)$  for the case  $\lambda^* < \lambda < \infty$ , showing the composition difference available to drive diffusion through the liquid ( $\Delta X$ ). (b) Model used to calculate the growth rate. 18

# Closer look at the tip of a growing dendrite

different from a planar interface because heat can be conducted away from the tip in three dimensions.

Assume the solid is isothermal ( $T'_S = 0$ )

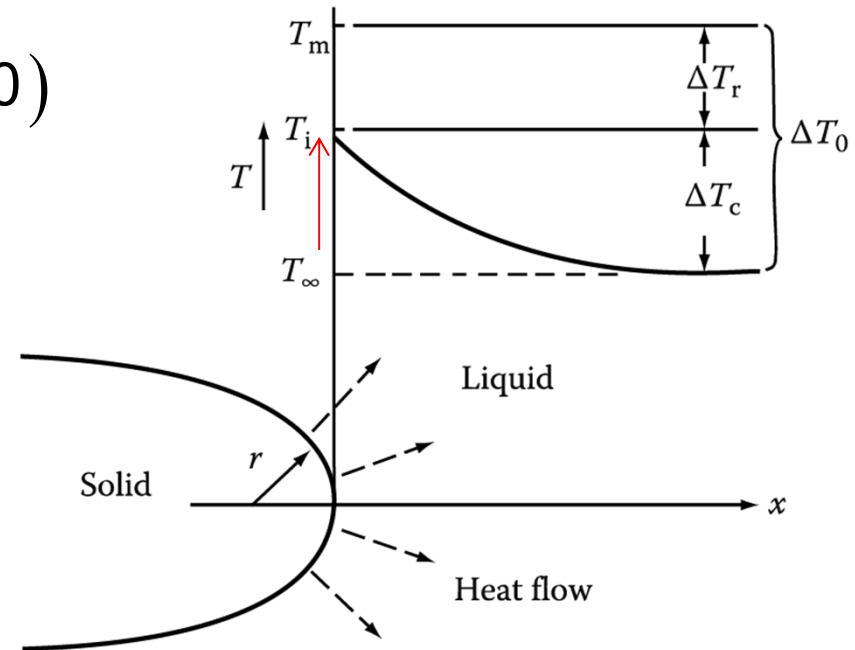
From  $K_S T'_S = K_L T'_L + v L_V$

If  $T'_S = 0$ ,  $v = \frac{-K_L T'_L}{L_V}$

A solution to the heat-flow equation for a hemispherical tip:

$$T'_L (\text{negative}) \cong \frac{\Delta T_C}{r} \quad \Delta T_C = T_i - T_\infty$$

$$v = \frac{-K_L T'_L}{L_V} \cong \frac{K_L}{L_V} \cdot \frac{\Delta T_C}{r} \quad v \propto \frac{1}{r}$$



However,  $\Delta T$  also depends on  $r$ .  
How?

## Thermodynamics at the tip?

Gibbs-Thomson effect:  
melting point depression

$$\Delta G = \frac{L_V}{T_m} \Delta T_r = \frac{2\gamma}{r} \quad \Delta T_r = \frac{2\gamma T_m}{L_V r}$$

## Minimum possible radius ( r )?

$$r_{min} : \Delta T_r \rightarrow \Delta T_0 = T_m - T_\infty \rightarrow r^*$$

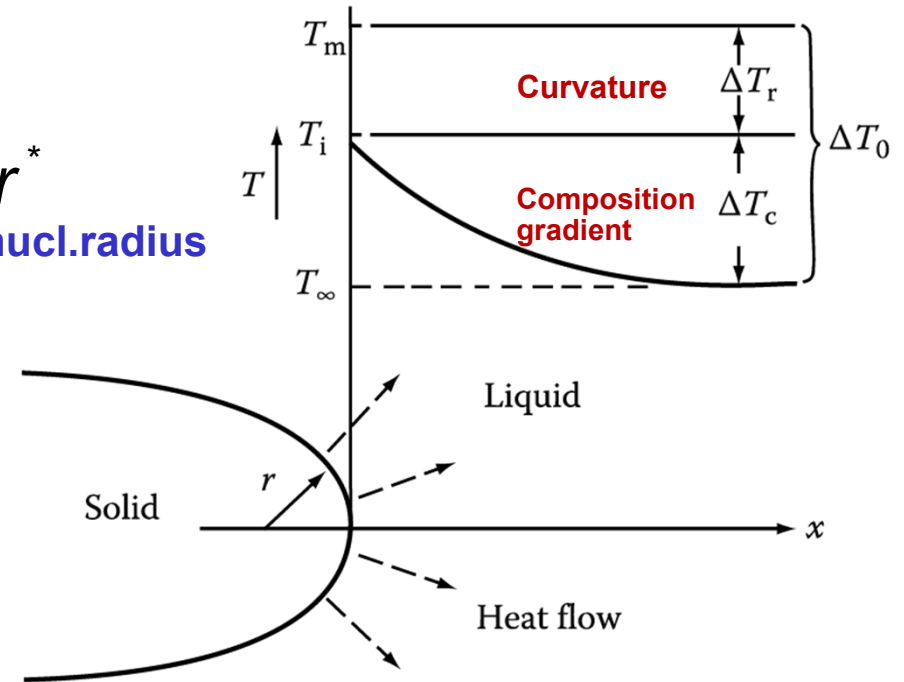
The crit.nucl.radius

$$r^* = \frac{2\gamma T_m}{L_v \Delta T_0}$$

$$\Delta T_r = \frac{2\gamma T_m}{L_v r}$$

Express  $\Delta T_r$  by  $r$ ,  $r^*$  and  $\Delta T_0$ .

$$\Delta T_r = \frac{r^*}{r} \Delta T_0$$



$$v \cong \frac{K_L}{L_v} \cdot \frac{\Delta T_c}{r} = \frac{K_L}{L_v} \cdot \frac{(\Delta T_0 - \Delta T_r)}{r} = \frac{K_L}{L_v} \cdot \frac{\Delta T_0}{r} \left( 1 - \frac{r^*}{r} \right)$$

$v \rightarrow 0$  as  $r \rightarrow r^*$  due to Gibbs-Thomson effect  
as  $r \rightarrow \infty$  due to slower heat conduction

Maximum velocity?

$$\rightarrow r = 2r^*$$

# Undercooling $\Delta T_0$

$$\Delta T_0 = \underbrace{\Delta T_r}_{\text{Curvature}} + \underbrace{\Delta T_D}_{\text{Composition gradient}} \quad \rightarrow \quad \Delta G_{total} = \underbrace{\Delta G_r}_{\text{Curvature}} + \underbrace{\Delta G_D}_{\text{Composition gradient}} \quad \rightarrow \quad v = k_2 D \frac{\Delta T_0}{\lambda} \left(1 - \frac{\lambda^*}{\lambda}\right)$$

$$\Delta G_r = \frac{2\gamma_{\alpha\beta} V_m}{\lambda}$$

$\rightarrow$  free energy dissipated in forming  $\alpha/\beta$  interfaces

$\Delta G_D \rightarrow$  free energy dissipated in diffusion

By varying the interface undercooling ( $\Delta T_0$ ) it is possible to vary the growth rate ( $v$ ) and spacing ( $\lambda$ ) independently.

Therefore, it is impossible to predict the spacing that will be observed for a given growth rate. **However, controlled growth experiments show that a specific value of  $\lambda$  is always associated with a given growth rate.**

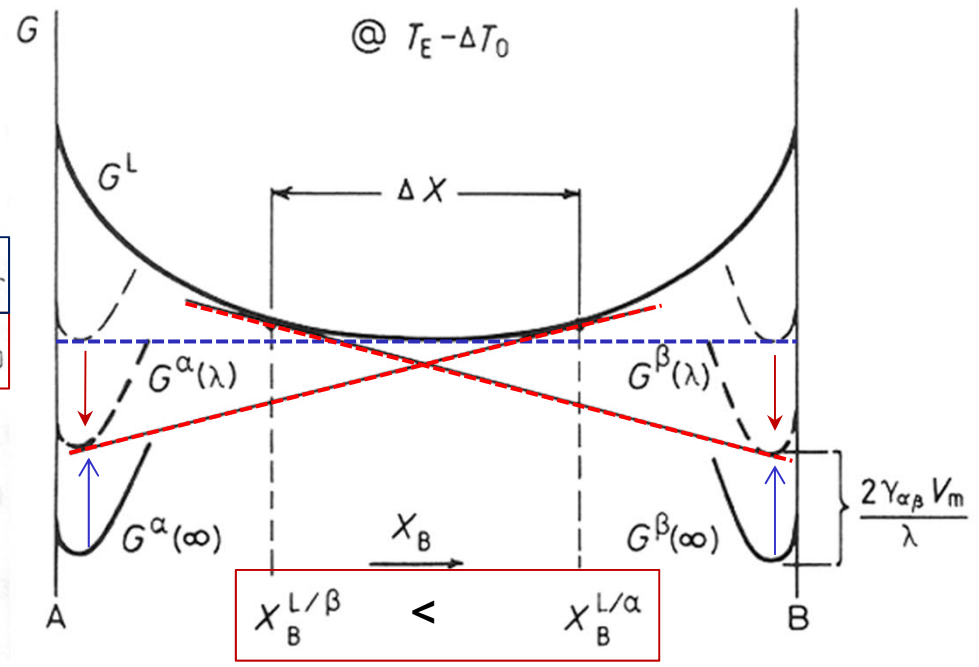
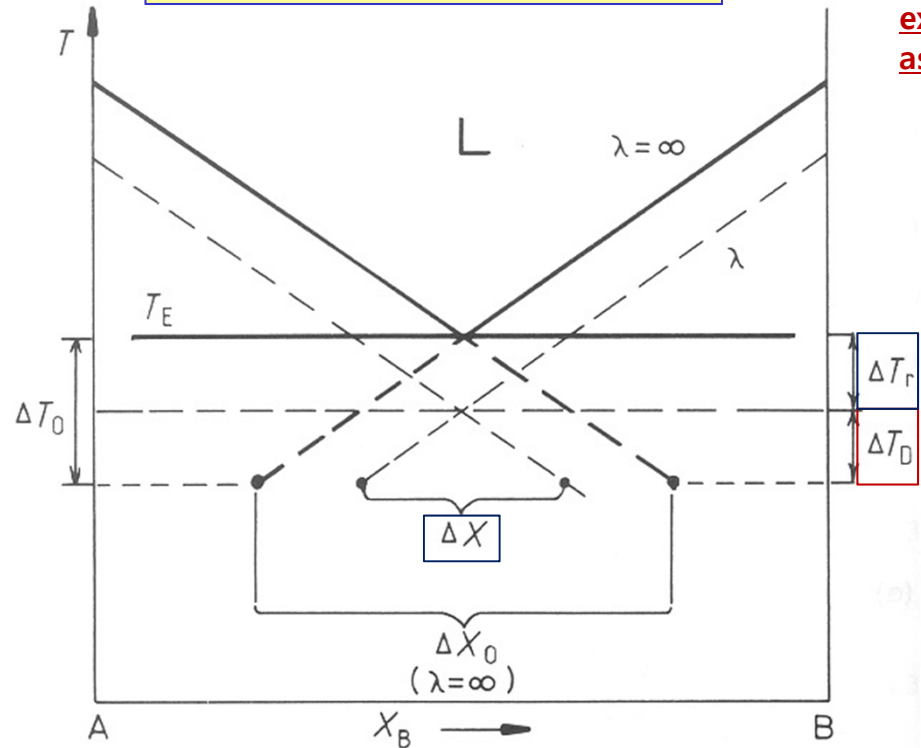
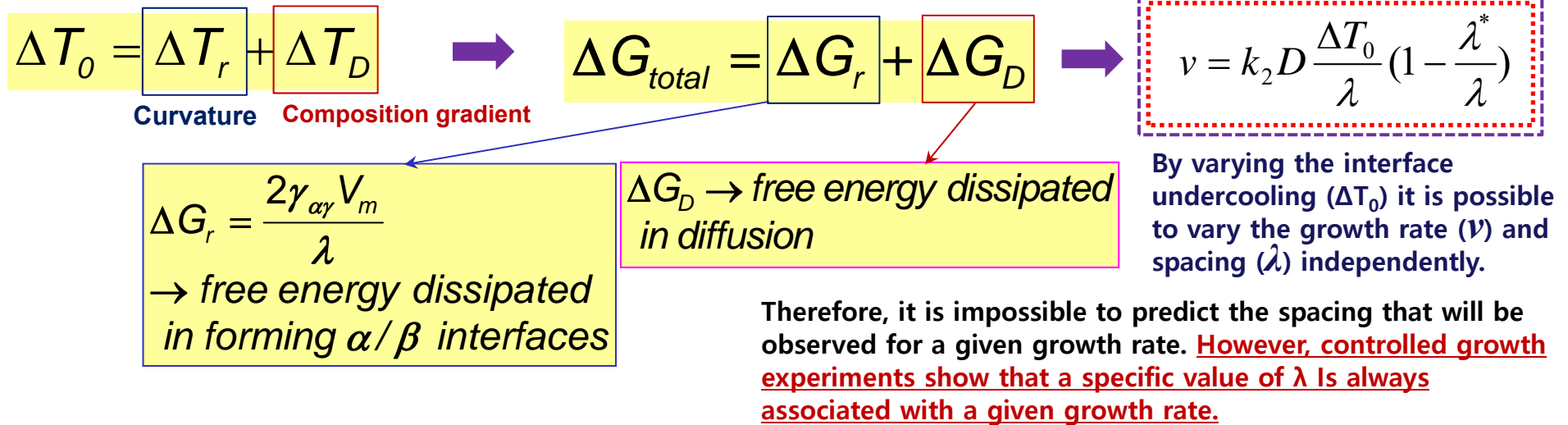


Fig. 4.34 Eutectic phase diagram showing the relationship between  $\Delta X$  and  $\Delta X_0$  (exaggerated for clarity)

# Undercooling $\Delta T_0$



\* For example,

Maximum growth rate at a fixed  $\Delta T_0 \rightarrow \lambda_0 = 2\lambda^*$

(4)  $v = k_2 D \frac{\Delta T_0}{\lambda} \left(1 - \frac{\lambda^*}{\lambda}\right)$  →  $v_0 = k_2 D \Delta T_0 / 4\lambda^*$  (5)

From Eq. 4.39

$\lambda^* = + \frac{2T_E \gamma V_m}{\Delta H \Delta T_0}$  →  $\Delta T_0 \propto 1/\lambda^*$  (6)

So that the following relationships are predicted:

(5) + (6) →

$v_0 \lambda_0^2 = k_3$  (constant)

$\frac{v_0}{(\Delta T_0)^2} = k_4$

Ex) Lamellar eutectic in the Pb-Sn system

$k_3 \sim 33 \mu\text{m}^3/\text{s}$  and  $k_4 \sim 1 \mu\text{m}/\text{s}\cdot\text{K}^2$

→  $v = 1 \mu\text{m}/\text{s}$ ,  $\lambda_0 = 5 \mu\text{m}$  and  $\Delta T_0 = 1 \text{ K}$

## \* Total Undercooling

$$\Delta T_0 = \Delta T_r + \Delta T_D$$

Undercooling required to overcome the interfacial curvature effects

Undercooling required to give a sufficient composition difference to drive the diffusion

Strictly speaking,

$\Delta T_i$  term should be added **but, negligible for high mobility interfaces**

Driving force for atom migration across the interfaces

$\Delta T_D \rightarrow$  Vary continuously from the middle of the  $\alpha$  to the middle of the  $\beta$  lamellae

$\Delta T_0 = \text{const}$   $\leftarrow$  Interface is essentially isothermal.

$\Delta T_D \rightarrow$   $\Delta T_r$  **The interface curvature will change across the interface.**

Should be compensated

## \* A planar eutectic front is not always stable.

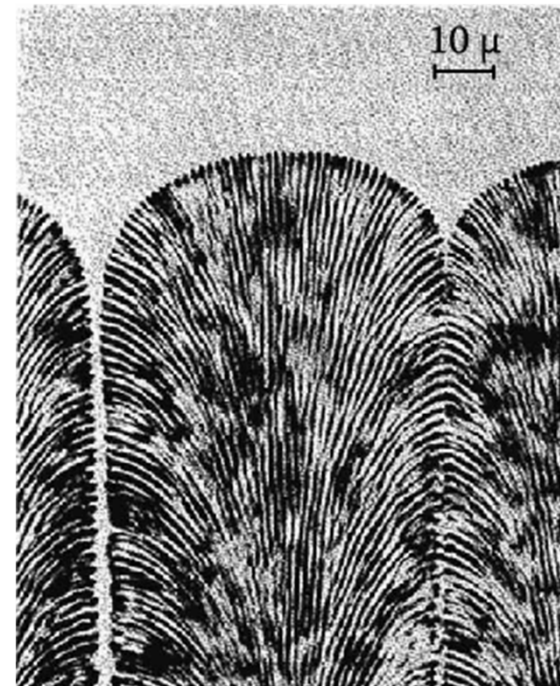
Binary eutectic alloys contains **impurities** or **other alloying elements**

**"Form a cellular morphology"**

$\rightarrow$  analogous to single phase solidification restrict in a sufficiently high temp. gradient.

$\rightarrow$  The solidification direction changes as the cell walls are approached and the lamellar or rod structure fans out and may even change to an irregular structure.

$\rightarrow$  **Impurity elements (here, mainly copper) concentrate at the cell walls.**



## A planar eutectic front is not always stable.

Binary eutectic alloys contains **impurities** or **other alloying elements**

“Form a cellular morphology”

→ analogous to single phase solidification restrict in a sufficiently high temp. gradient.

- The solidification direction changes as the cell walls are approached and the lamellar or rod structure fans out and may even change to an irregular structure.
- Impurity elements (here, mainly copper) concentrate at the cell walls.

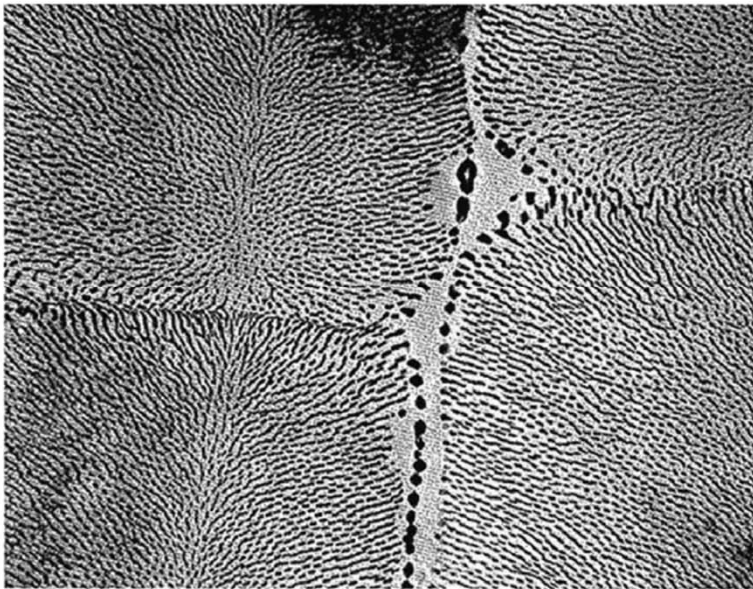
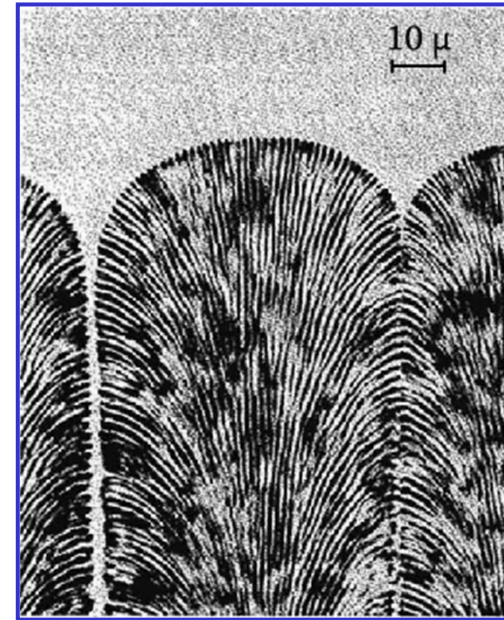


Fig. 4.35 Transverse section through the cellular structure of an Al-Al<sub>6</sub>Fe rod eutectic (x3500).

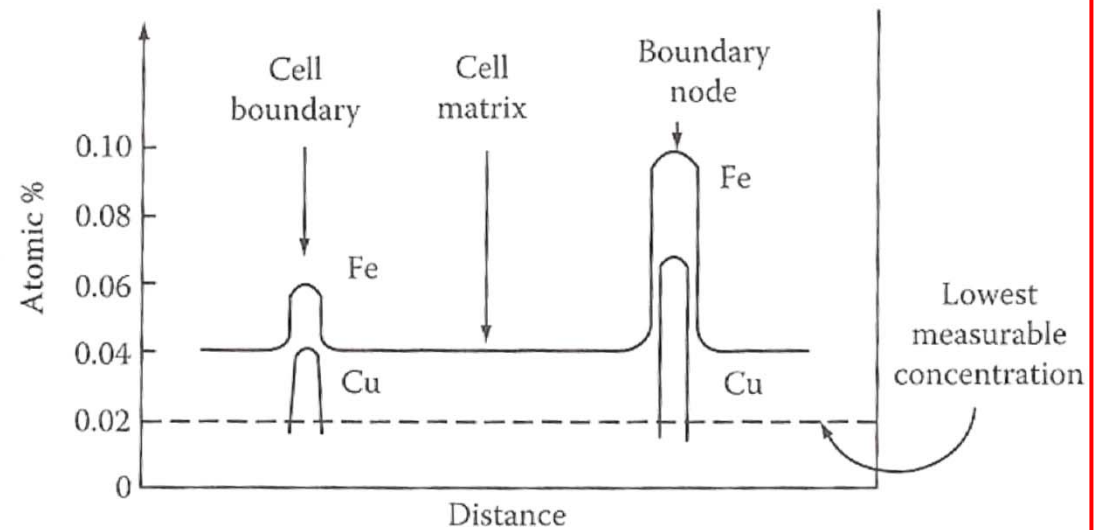


Fig. 4.36 Composition profiles across the cells in Fig. 4.35b.

## An alternative approach for lamellar growth by Jackson and Chalmers,

Terminating layer T  
by change of speed of growth

The stability of the tip T is the criterion  
for the stable lamellar width,  $\lambda$ .

Assumption:

- 1) interface ~ isothermal
- 2) Total supercooling of interfaces  
~ sum of the supercooling due to curvature
- 3) the enrichment of the liquid in contact  
with the interface by rejection of the solute

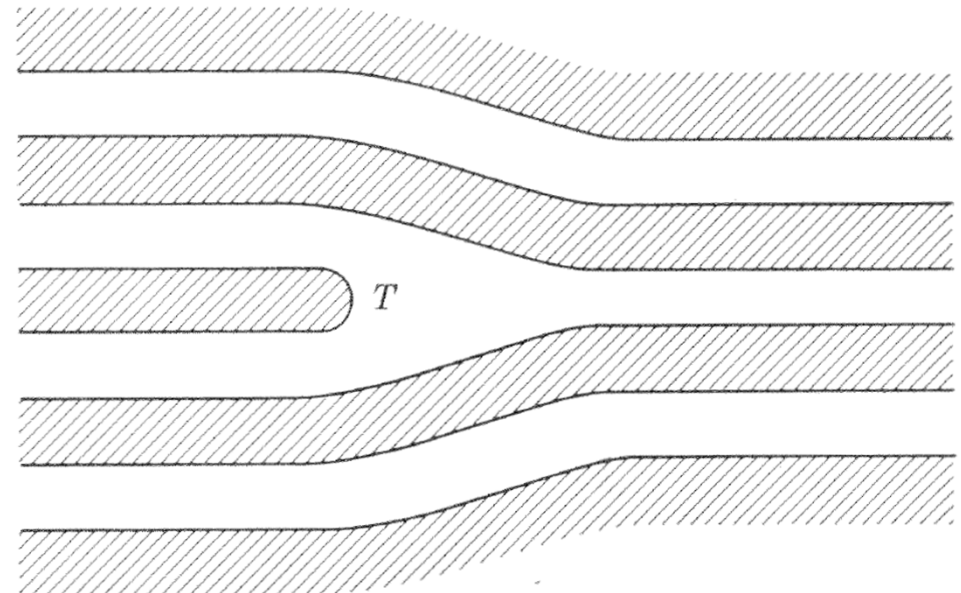
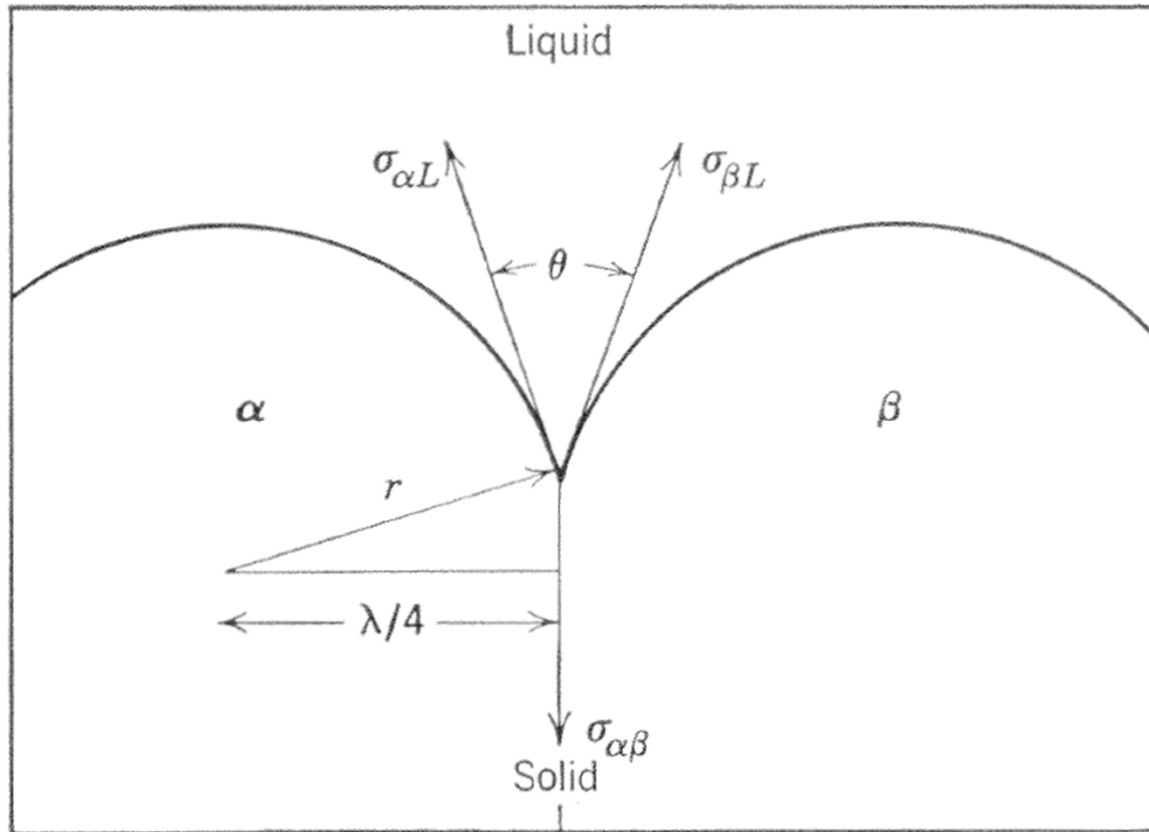


Fig. 6.16. Termination of lamellar (schematic)

The supercooling is calculated 1) at the intersection of a termination with the interface, and 2) at a position remote from terminations.

- Assumptions: 1) Width of two lamellar ~ equal  
 2) Curvature ~ uniform and equal  
 3) Surface free energies of the two phases ( $\alpha$  and  $\beta$ ) ~ equal



$$2\sigma_{\alpha L} \cos \frac{\theta}{2} = \sigma_{\alpha\beta}$$

$$\frac{\lambda}{4} = r \cos \frac{\theta}{2}$$

$$\cos \frac{\theta}{2} = \frac{\sigma_{\alpha\beta}}{2\sigma_{\alpha L}} = \frac{\lambda}{4r}$$

$$\frac{\sigma_{\alpha L}}{r} = \frac{2\sigma_{\alpha\beta}}{\lambda}$$

Fig. 6.17. Region of interface near the junction of two lamellae.

Diffusion of solute  
 ahead of the interface

$$(C_{\alpha}^L - C_E) = [(1 - k_{\alpha})C_E R \lambda] / 8D$$

$$\Delta T_c = [(1 - k_{\alpha})C_E R \lambda m_{\alpha}] / 8D \quad m : \text{slope of liquidus line}$$

Supercooling at curvature center

$$\Delta T_r = \frac{\sigma_{\alpha L} T_E}{Lr} \quad \text{but} \quad \frac{\sigma_{\alpha L}}{r} = \frac{2\sigma_{\alpha\beta} T_E}{L\lambda}$$

and therefore

$$\Delta T_r = \frac{2\sigma_{\alpha\beta} T_E}{L\lambda}$$

At termination point T, Curvature change (cylindrical → Spherical)  $\Delta T_r = 4\sigma_{\alpha\beta} T_E / L\lambda$

Amount of solute rejected by the half cylinder of the termination (assumed to be stable),

$$(1 - k_{\alpha}) C_E R (\pi/2) (\lambda^2/16) \quad \text{per unit time}$$

Amount of solute diffuses across the semicircular interphase boundary

$$(1 - k_{\alpha}) C_E R \frac{\pi}{2} \frac{\lambda^2}{16} = \frac{D(C_{\alpha}^L - C_E) \lambda / 2}{\lambda/4} \pi \frac{\lambda}{4}$$

or

$$C_{\alpha}^L - C_E = \frac{(1 - k_{\alpha}) C_E R \lambda}{16D}$$

from which

$$\Delta T_c = \frac{m_{\alpha} (1 - k_{\alpha}) C_E R \lambda}{16D}$$

The sums of the two supercoolings are equated, giving

$$\lambda^2 R = \frac{32\sigma_{\alpha\beta} T_E D}{m_{\alpha} (1 - k_{\alpha}) C_E L}$$

from which  $\lambda^2 R$  is a constant, or,  $\lambda \propto R^{-1/2}$ .

## 5) Lamellar growth: experimental

Al-Zn, Al-Cu, Al-Zn, Pb-Sn, Pb-Cd  
good agreement

$$v_0 \lambda_0^2 = k_3 \text{ (constant)}$$

$$\frac{v_0}{(\Delta T_0)^2} = k_4$$

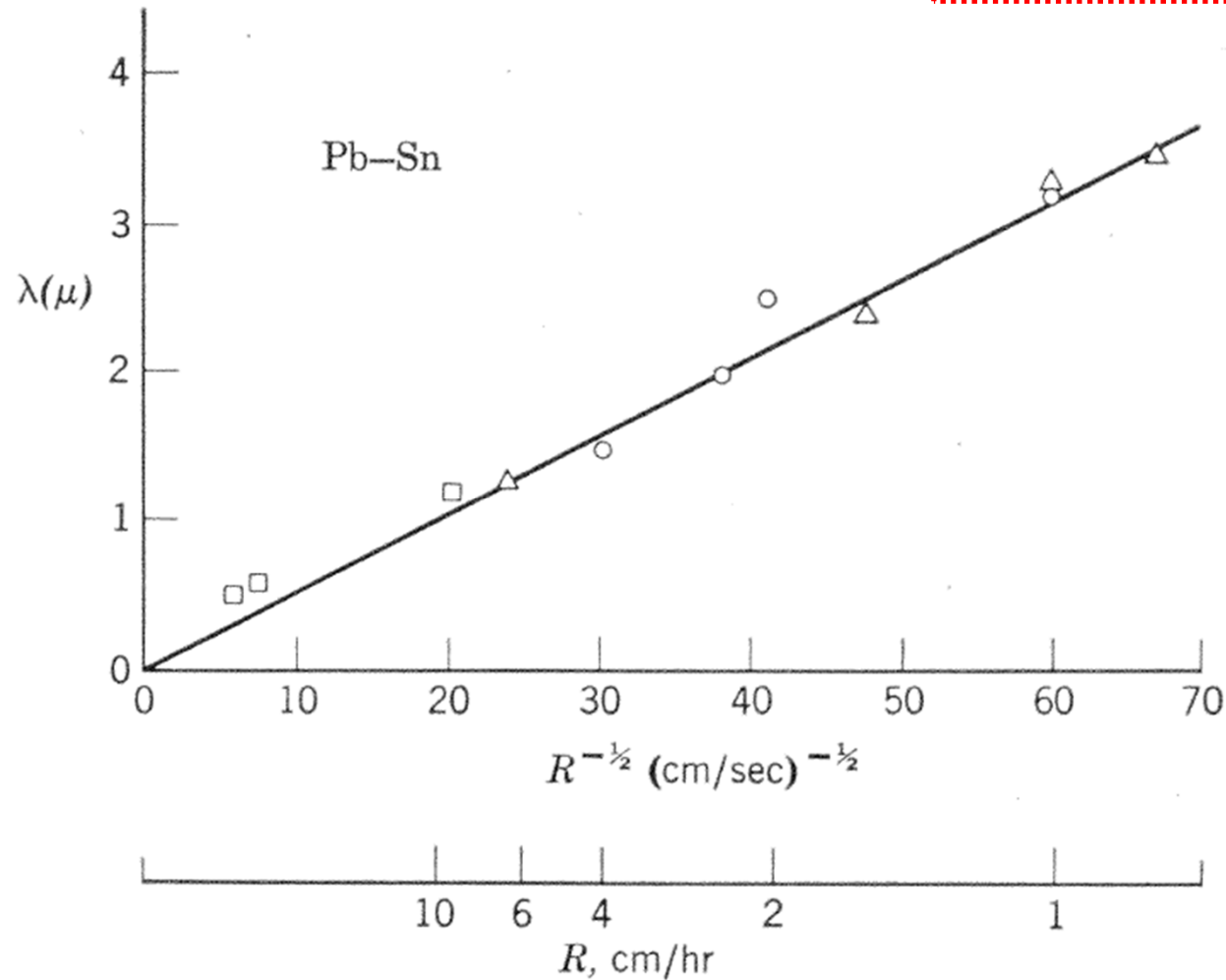


Fig. 6.18. Relationship between interlamellar spacing and growth rate for the lead-tin eutectic.

## 5) Lamellar growth: experimental

Al-Zn, Al-Cu, Al-Zn, Pb-Sn, Pb-Cd  
good agreement

$$v_0 \lambda_0^2 = k_3 \text{ (constant)}$$

$$\frac{v_0}{(\Delta T_0)^2} = k_4$$

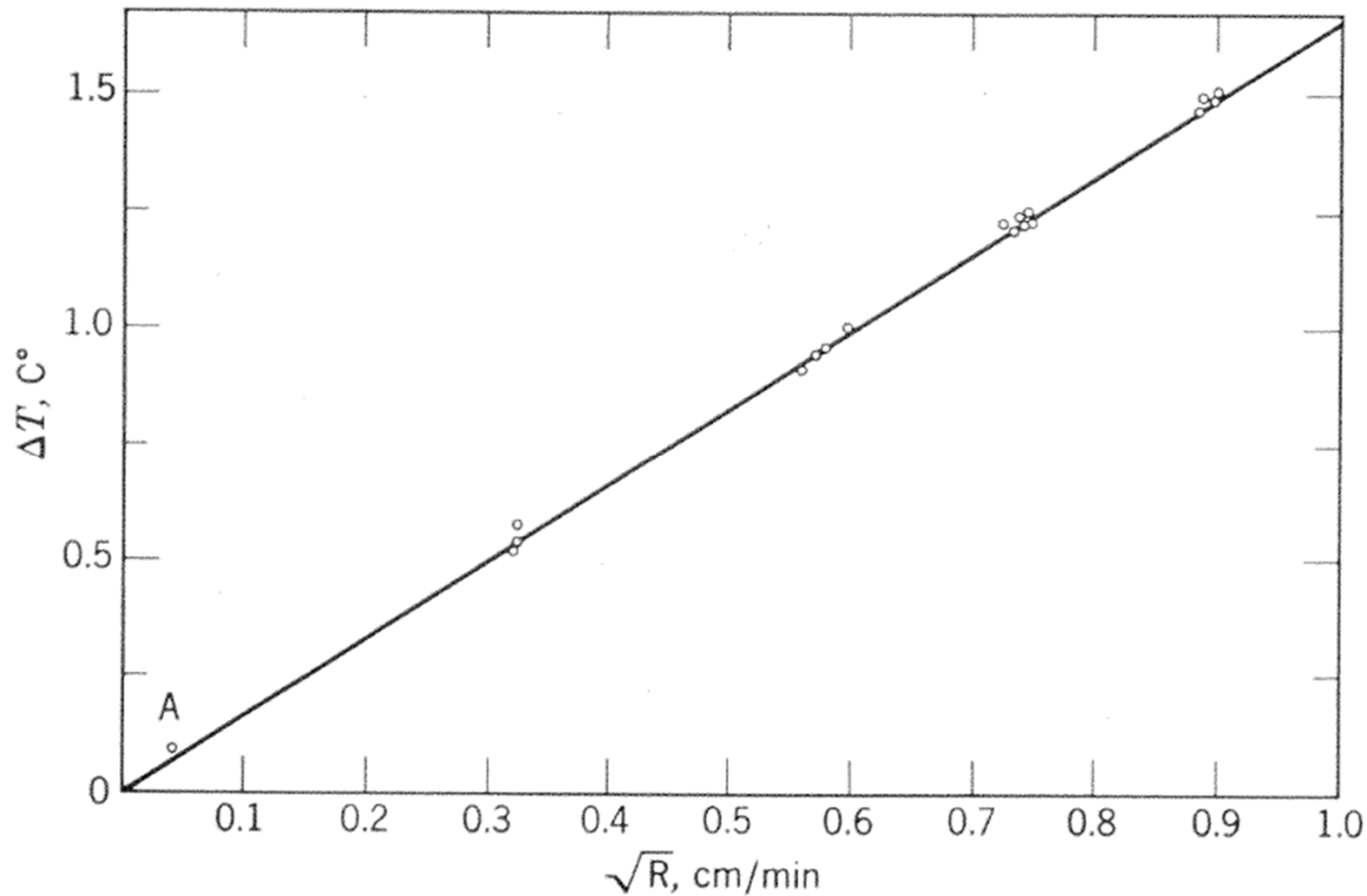


Fig. 6.19. Supercooling of eutectic interface as a function of growth rate (lead-tin).

## 6) Degenerate eutectic structure

Pure eutectic (lamellar type) ~ a very wide range of solidification rate

→ structure degenerate at very slow rates of solidification (less than 1cm/hr)

\* Degenerate structure: resemble the beginning of the spheroidization process that occurs during prolonged annealing

→ But, the degenerate structure is formed during, and not after, solidification.

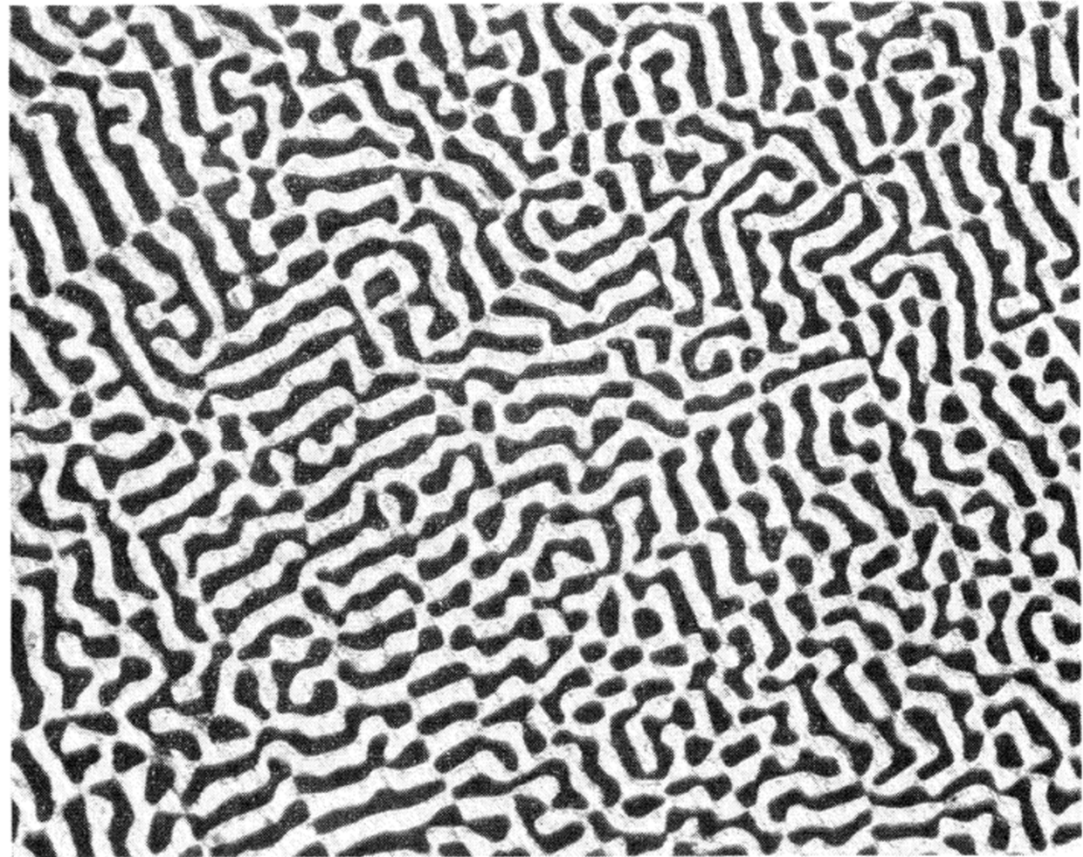


Fig. 6.20. Degenerate eutectic structure in CuAl<sub>2</sub>-Al eutectic at 0.8 cm/hr (X500).

## 7) Modification of Eutectics

Two degenerate forms of the lamellar structure by impurities

→ (a) Colony structure and (b) Rod structure

(a) Colony structure

: a cellular structure superimposed on the lamellar eutectic structure

\* An impurity or an excess of one constituent, would diffuse much farther ahead of the interface than would be required for transverse interlamellar diffusion

→ The long range diffusion sets up constitutional supercooling → Cell formation and the resulting transverse diffusion of the impurity

→ if purity of the eutectic were sufficiently high, the colony structure are eliminated (regular lamellar structure is produced)

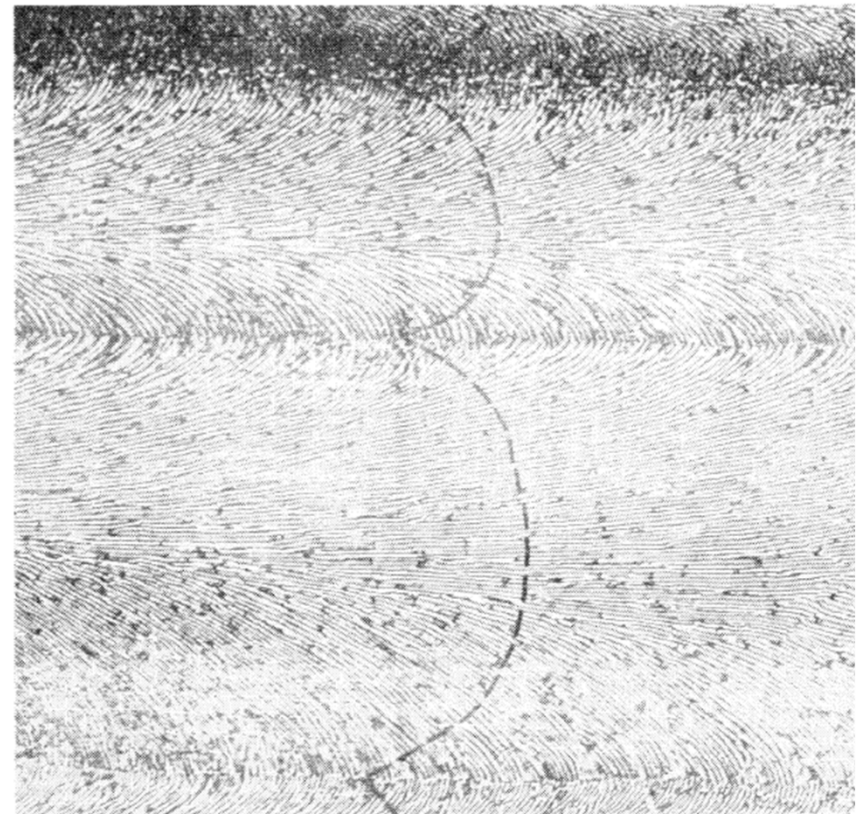


Fig. 6.21. Longitudinal section of impure CuAl<sub>2</sub>-Al eutectic alloy. Broken line indicates shape of interface during growth.

# A planar eutectic front is not always stable.

Binary eutectic alloys contains **impurities** or **other alloying elements** →

Form a **cellular morphology** analogous to single phase solidification Restrict in a sufficiently high temp. gradient.

- The solidification direction changes as the cell walls are approached and the lamellar or rod structure fans out and may even change to an irregular structure.
- Impurity elements (here, mainly copper) concentrate at the cell walls.

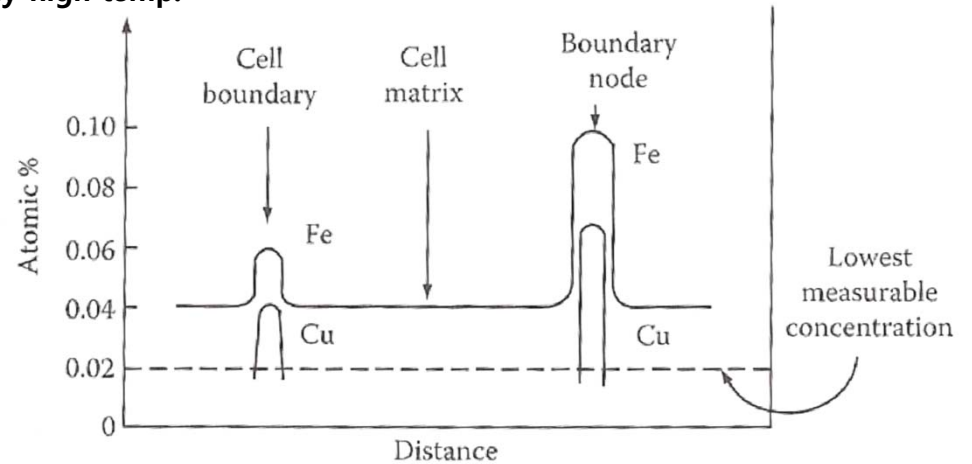


Fig. Composition profiles across the cells

\* Total Undercooling  $\Delta T_0 = \Delta T_r + \Delta T_D$

Undercooling required to overcome the interfacial curvature effects

Undercooling required to give a sufficient composition difference to drive the diffusion

Strictly speaking,

$\Delta T_i$  term should be added **but, negligible for high mobility interfaces**

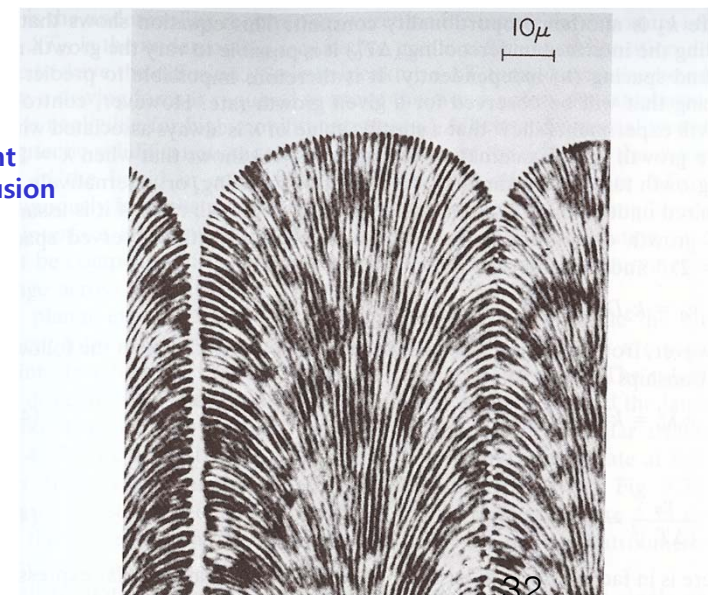
Driving force for atom migration across the interfaces

$\Delta T_D \rightarrow$  Vary continuously from the middle of the  $\alpha$  to the middle of the  $\beta$  lamellae

$\Delta T_0 = const \leftarrow$  Interface is essentially isothermal.

$\Delta T_D \rightarrow \Delta T_r$  The interface curvature will change across the interface.

Should be compensated



(b) Rod structure

: Impurity has sufficiently different distribution coefficients for the two solid phases

\* When the two distribution coefficient are very different, the lamellae of one phase should grow into the liquid ahead of the other, and the lamellae of the lagging phase then break up into very small cells, separated by the other phase.

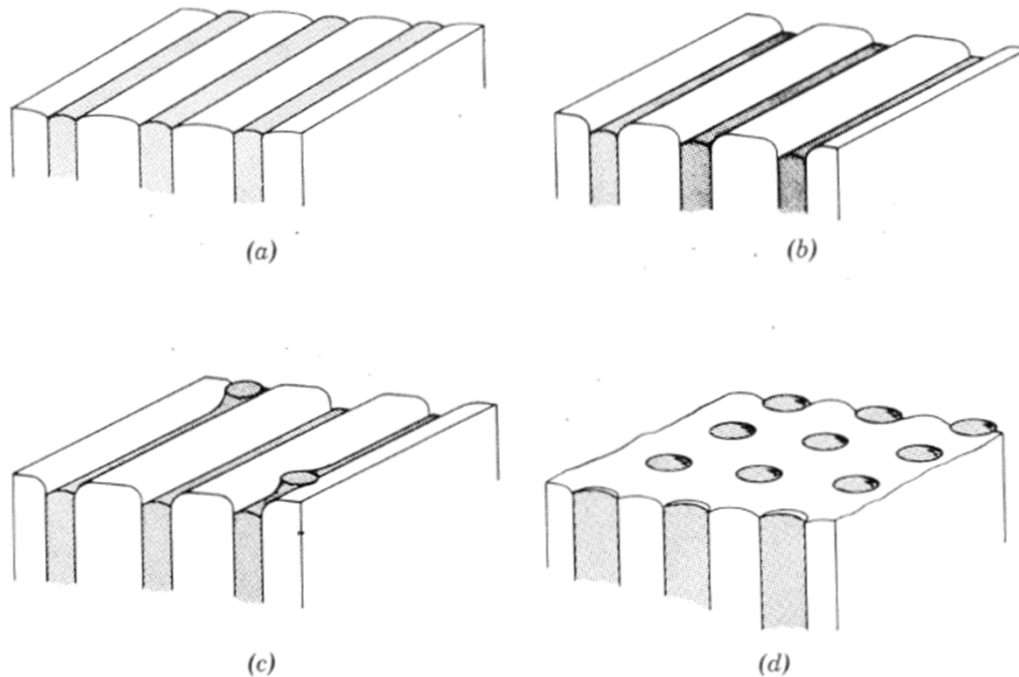


Fig. 6.22. Origin of “rod-type” eutectic structure (schematic).

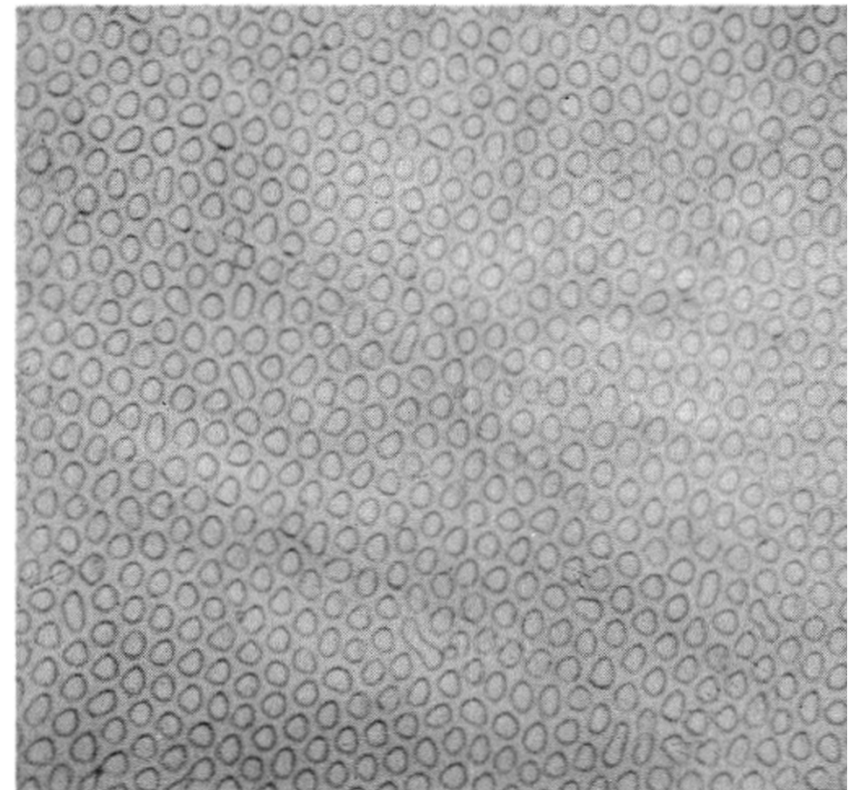


Fig. 6.23. Cross section of “rod-type” eutectic structure.

(C) Intermediate structure: Middle= lamellar structure/ edge = rod-type colony

: This is caused by an impurity which when present at a low concentration, has nearly equal distribution coefficient for the two solid phases, but which has increasingly differing distribution coefficients as its concentration increases.

\* Middle part of Cell

: relatively low concentration & similar distribution coefficients

→ Lamellar structure

\* Edge of cell (near wall)

: relatively high concentration & sufficient distribution coefficients

→ Rod-type structure

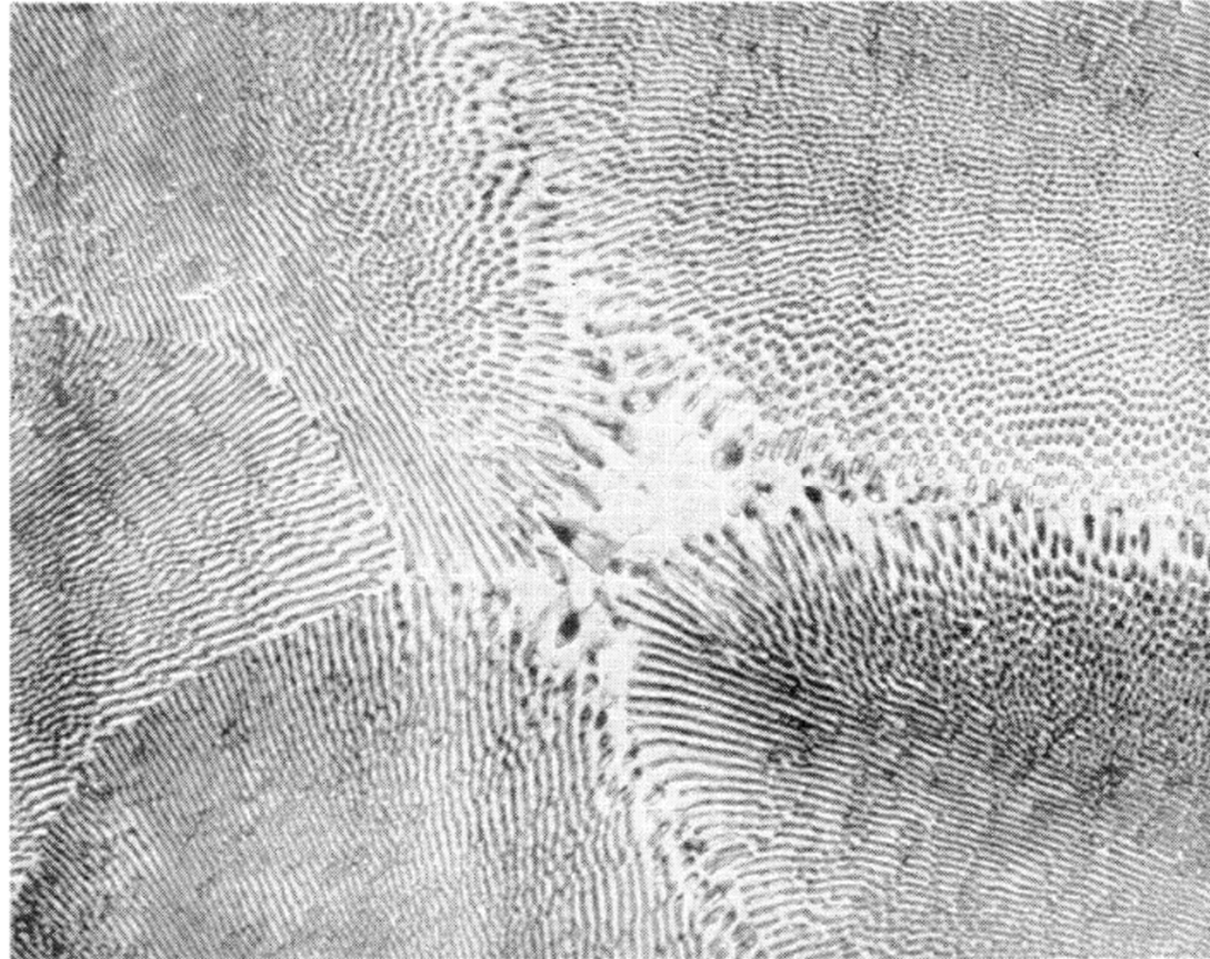


Fig. 6.24. "Mixed lamellar and rod structure" (Pb-Cd eutectic alloy with 0.1% Sn)

## (d) Discontinuous eutectic structure

In lamellar type & degenerate form, each phase grows continuously  
→ does not required repeated nucleation.

“Discontinuous eutectic” : required renucleate repeatedly due to “strong anisotropy”  
of growth characteristics of one of the phases

a) Case I: both phases renucleate repeatedly due to the termination of growth of crystals



Fig. 6.25. “Chinese script” structure in Bi-Sn eutectic alloy

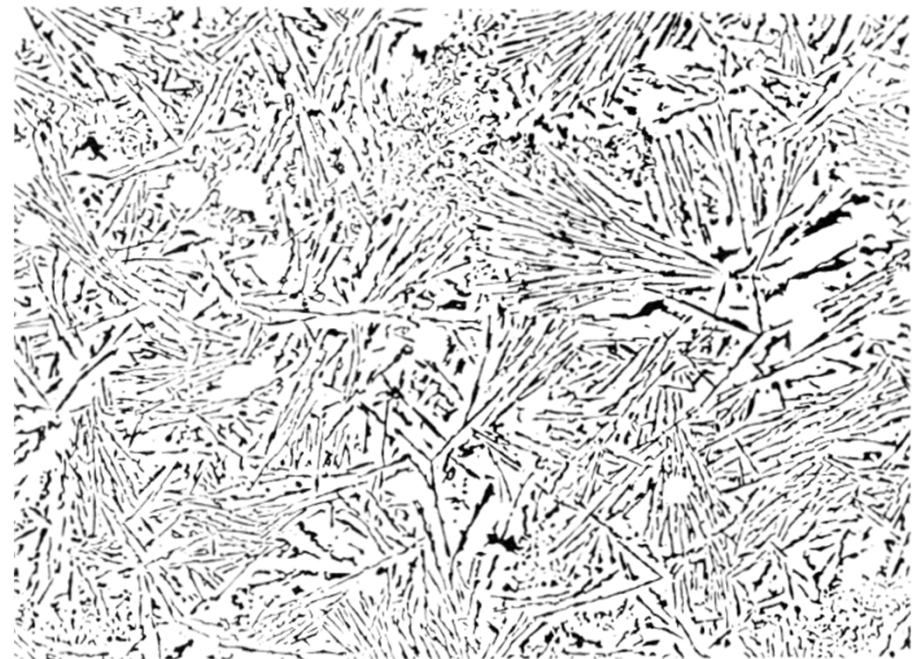


Fig. 6.26. Microstructure of Al-Si eutectic alloy.

## (d) Discontinuous eutectic structure

: required renucleate repeatedly due to “strong anisotropy” of growth characteristics

a) Case I: both phases renucleate repeatedly due to the termination of growth of crystals

\* Typical discontinuous eutectic type growth mechanism (Figure 6.26)

- Random nucleation and growth independent with growth interface

-  $I_1$ : three Si phases (A, B, C) growth  
B = block of growth of C  
A & B distance increase

$I_2$ : Nucleation and growth of D

- Chinese script (Fig. 6.25) type has not been investigated sufficiently.

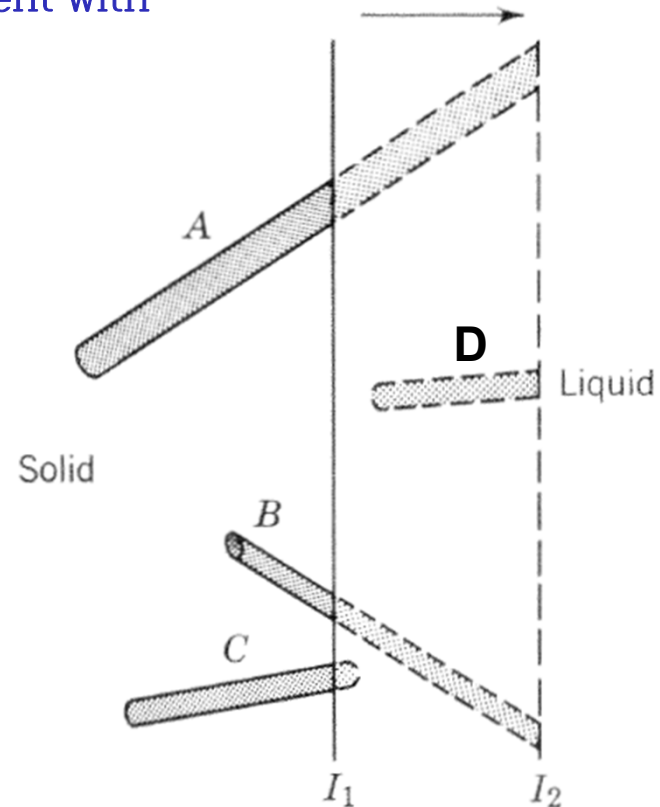


Fig. 6.27. Growth of a discontinuous eutectic (schematic), showing two positions of the interface ( $I_1$  and  $I_2$ ).

## (d) Discontinuous eutectic structure

b) “Spiral type of discontinuous eutectic” - Al-Th & Zn-Mg alloys

: one or both of the phases → anisotropic in growth rate

→  $\alpha$  phase grows faster than the  $\beta$  phase in one direction and more slowly in the other (unusual structure in Fig. 6.30).

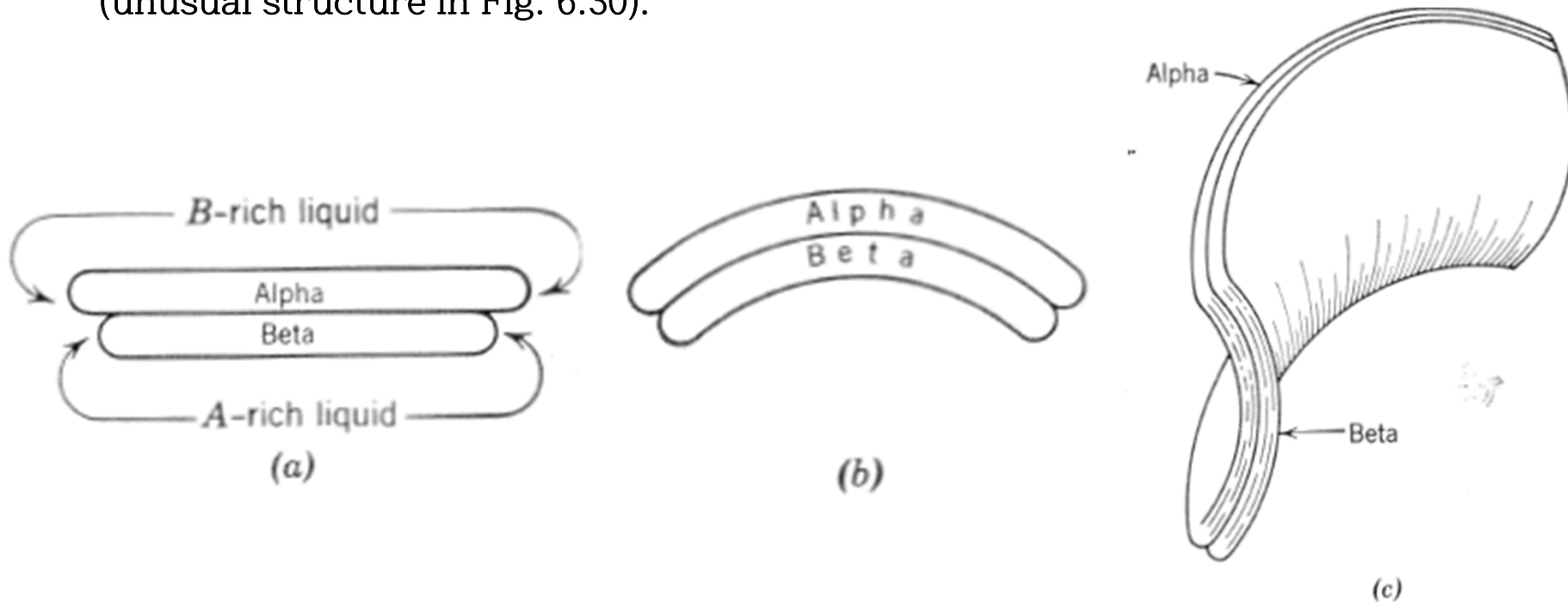


Fig. 6.30. Origin of spiral eutectic (schematic).

## (d) Discontinuous eutectic structure

b) “Spiral type” discontinuous eutectic” - Al-Th & Zn-Mg alloys

: one or both of the phases  $\rightarrow$  anisotropic in growth rate

\* If the two edges of the  $\beta$  phase do not form a closed ring, but overlap, then a spiral will be formed in that plane, and the complete structure will develop into a double conical spiral as shown in Fig. 6.29.

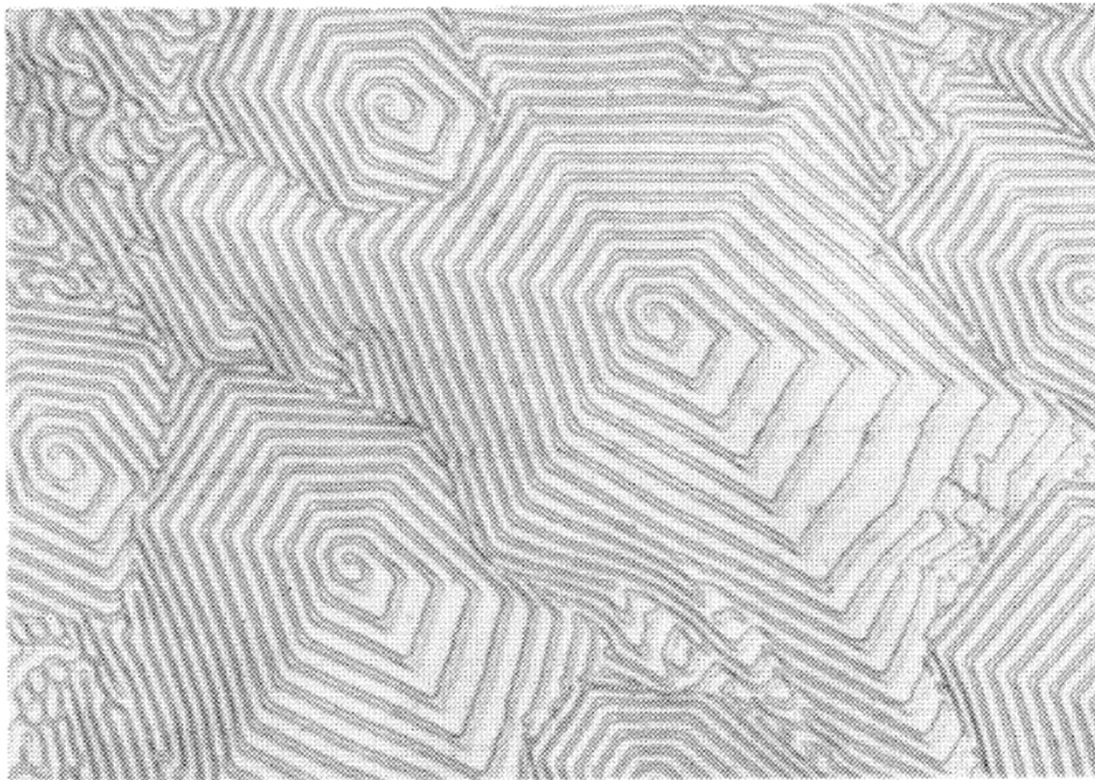


Fig. 6.28. Spiral eutectic structure in Zn-Mg alloy.

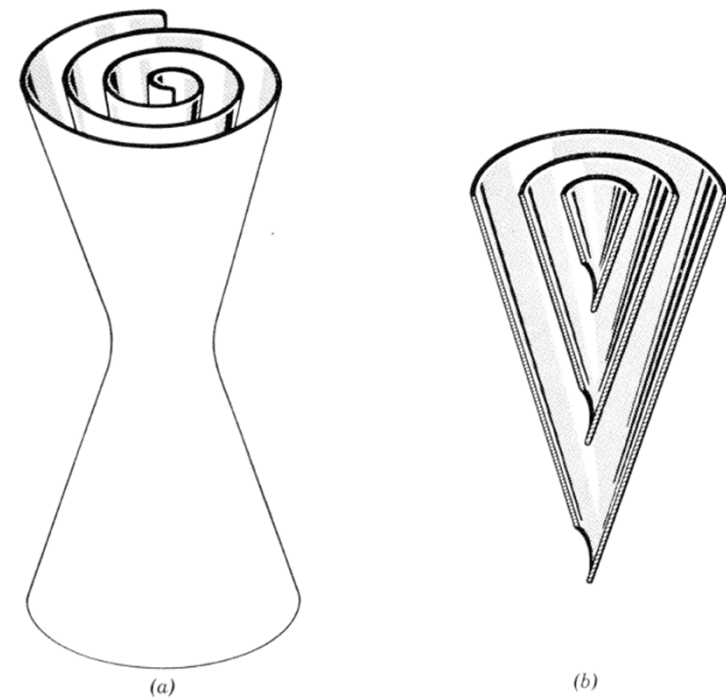


Fig. 6.29. Detailed structure of the spiral eutectic (schematic).

## (e) Special cases of the modification of eutectics

Ex) Microstructure of Al-Si eutectic could be modified by the minor addition of solutes:

① Addition of 0.01 % Sodium

Needle or plate type Si morphology → very smaller, more spherical Si particles

② Rapid Cooling → very smaller, more spherical Si particles

\* An explanation for these phenomena

→ the modified structure is formed at a temp. a few degrees below the normal  $T_e$ .

① Modifier changes the surface tension relationships (due to lower latent heat and higher thermal conductivity of Al) → very smaller, more spherical Si particles

② Rapid quenching →

due to thermal difference로

→ Large supercooling

a. decrease of Si precipitation (follows EA line)

b. decrease of  $r^*$  of Si and constantly  
renucleating Si

→ very smaller, more spherical Si particles

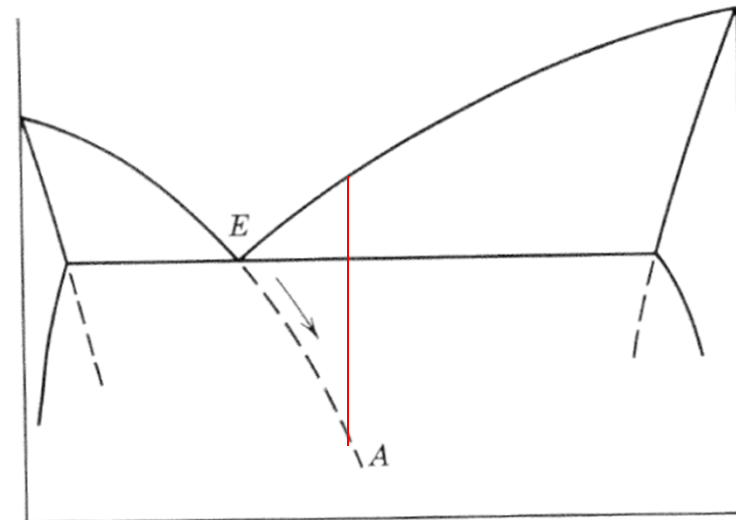


Fig. 6.31. Supercooling of eutectic in the absence of the second phase.

## 8) Non-eutectic composition

Solidification of  $C_0$  liquid

① complete mixing: Primary  $\alpha$   $C_s \rightarrow C_T$   
Liquid 조성  $C_0 \rightarrow E$

② less complete mixing: primary solidification

Depending on undercooling: Cellular  $\rightarrow$   
Cellular-dendritic  $\rightarrow$  New crystal nuclei

In real cases, the terminal transient liquid is far richer in solute than would be predicted from the equilibrium diagram, and it is therefore difficult to avoid the formation of some eutectic if the relevant liquid line terminates at a eutectic point.

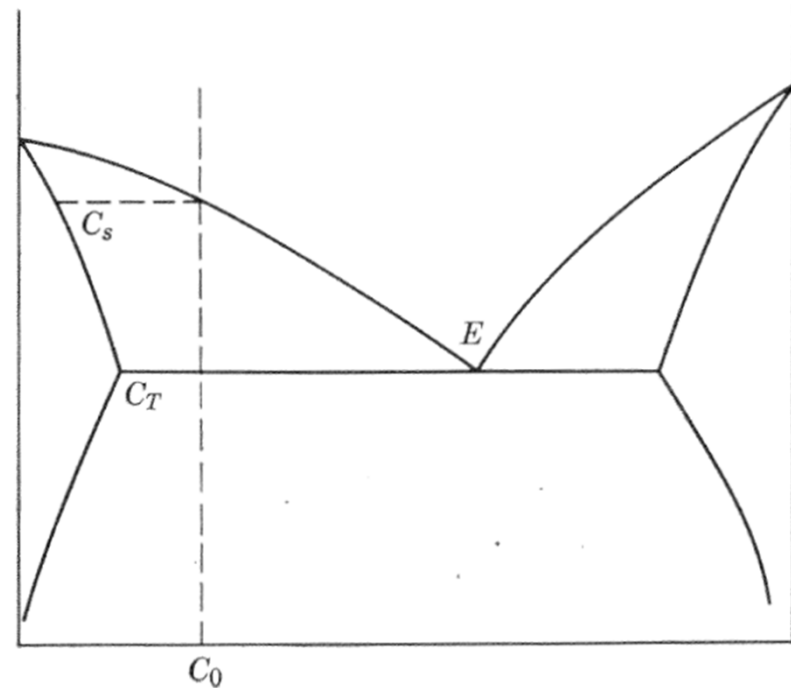
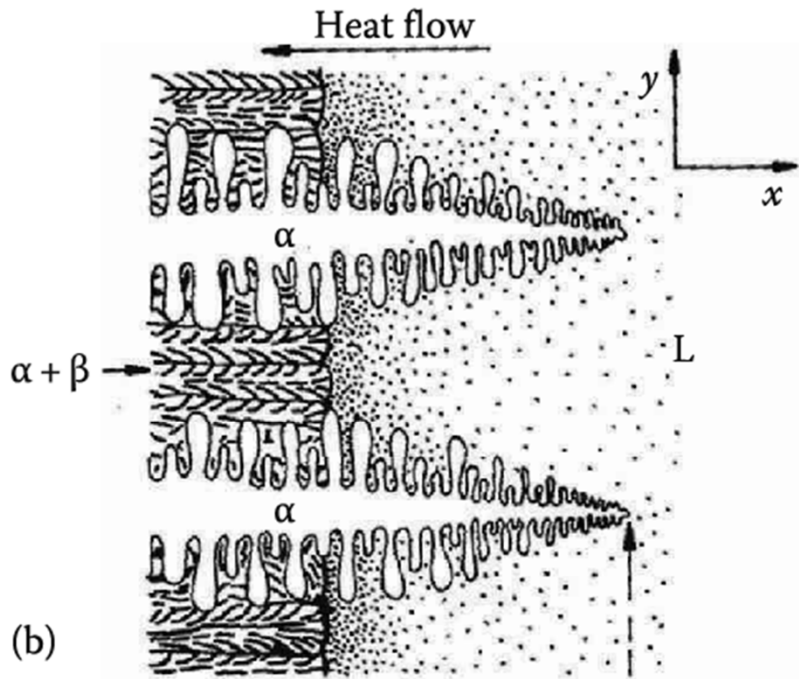


Fig. 6.32. Solidification of a eutectic system at a non-eutectic composition.

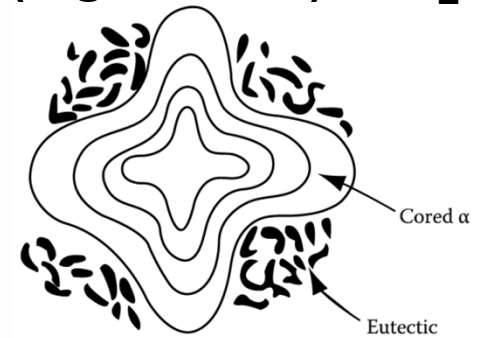
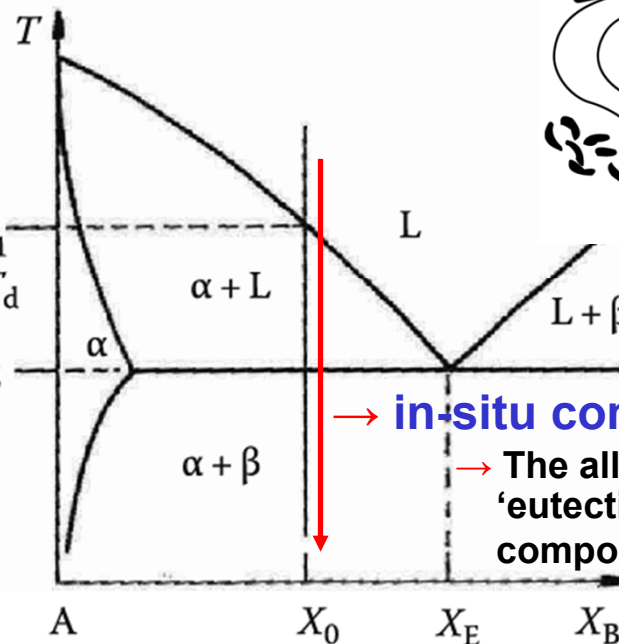
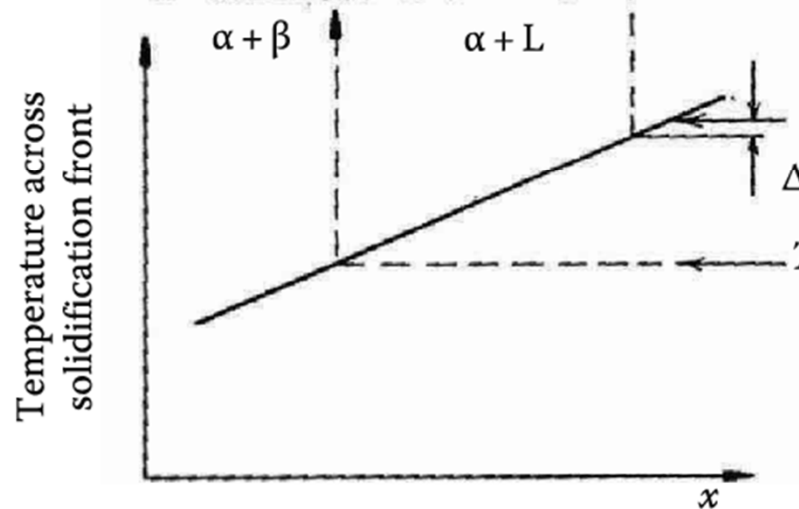
# \* Off-eutectic Solidification



**primary  $\alpha$  + eutectic lamellar**

- Primary  $\alpha$  dendrites form at  $T_1$ . Rejected solute increases  $X_L$  to  $X_E$ ; eutectic solidification follows.

- **Coring**: primary  $\alpha$  (low solute) at  $T_1$  and the eutectic (high solute) at  $T_E$ .



→ **in-situ composite materials**

→ The alloy solidifies as 100% 'eutectic' with an overall composition  $X_0$  instead of  $X_E$ .

(c)

(a)

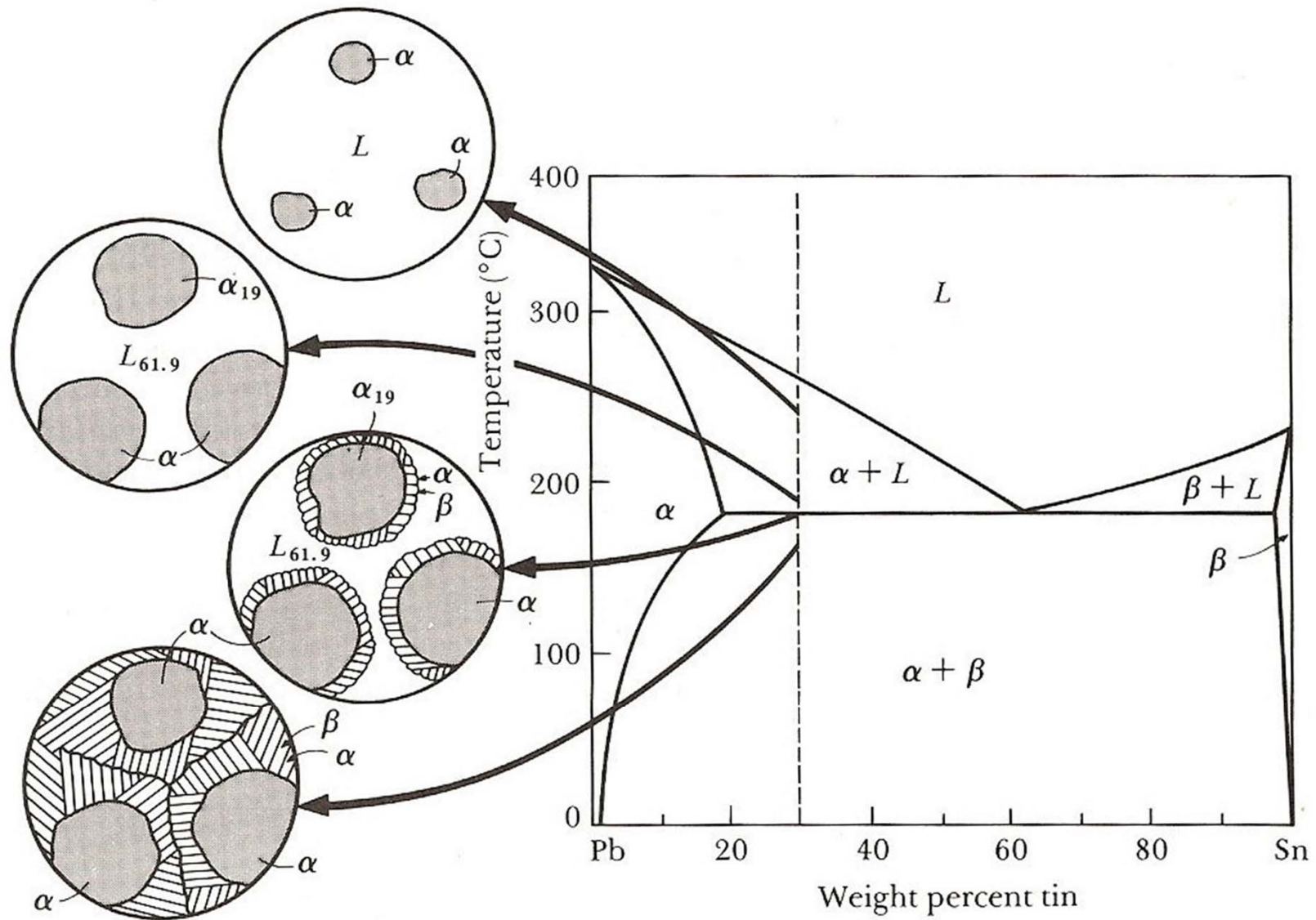
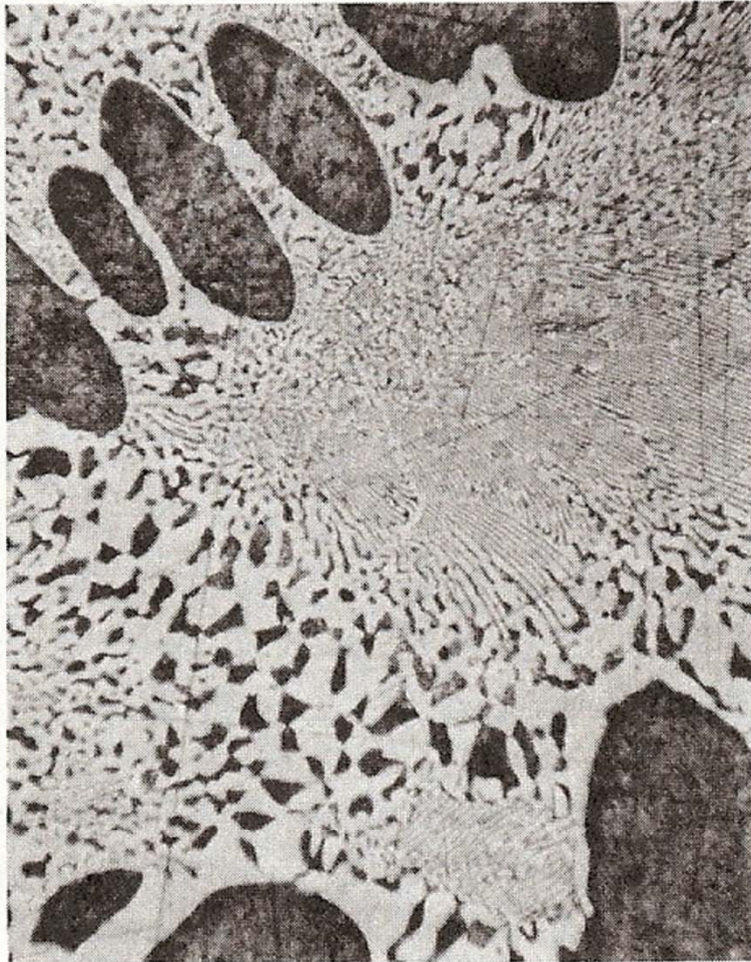
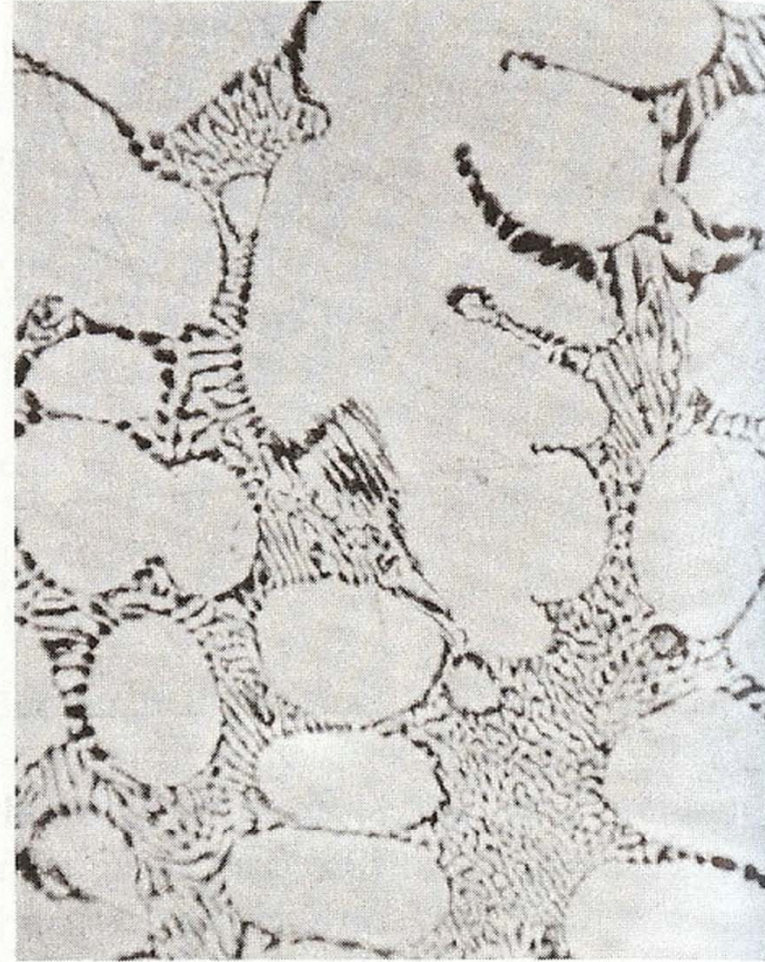


**FIGURE 10-12** The solidification and microstructure of a hypoeutectic alloy (Pb-30% Sn).



(a)



(b)

**FIGURE 10-13** (a) A hypoeutectic lead-tin alloy. (b) A hypereutectic lead-tin alloy. The dark constituent is the lead-rich solid  $\alpha$ , the light constituent is the tin-rich solid  $\beta$ , and the fine plate structure is the eutectic ( $\times 400$ ).

## 9) Gravity segregation of eutectic

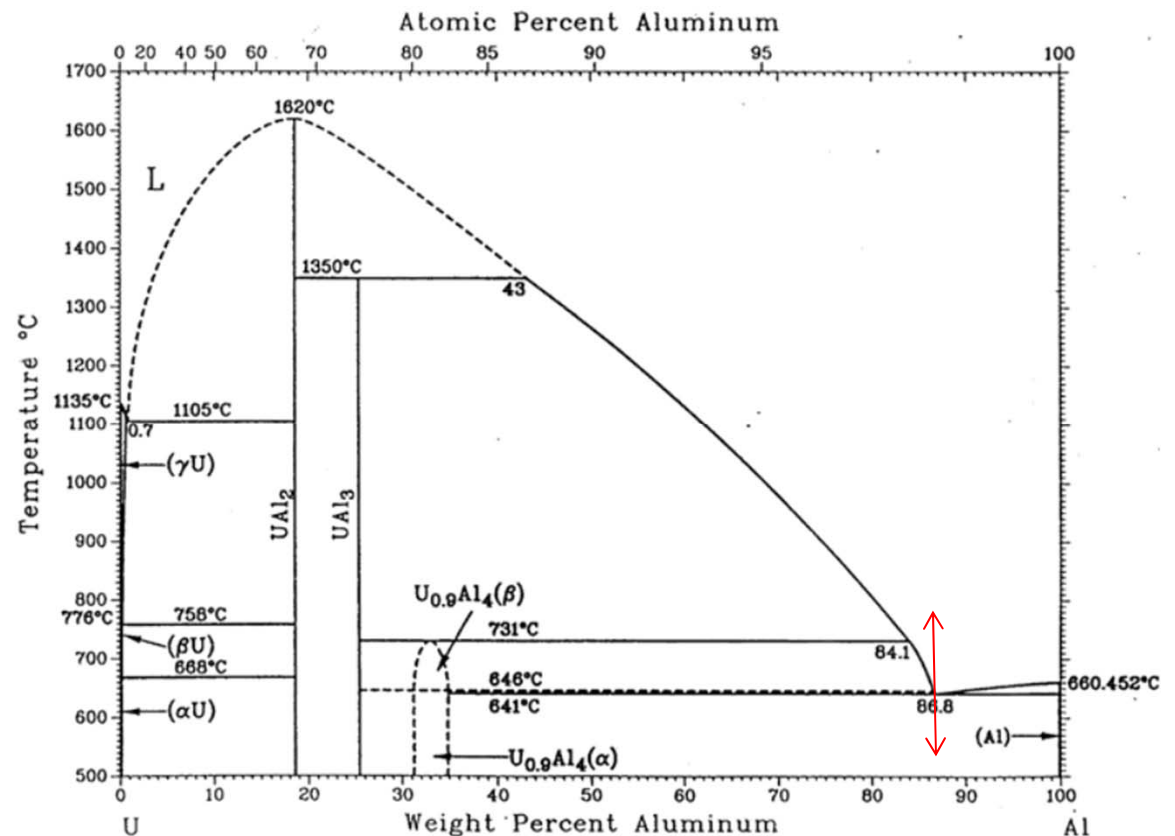
\* Uranium-Al eutectic region: “Cycled” up and down of  $T_E$

→ **marked segregation:** crucible bottom\_U concentration  $\uparrow$  / top: Al concentration  $\uparrow$

→ **Degree of Segregation :** depending on # of Cycles

Ex) Al-13.3 wt% U → 168 cycles → **bottom 45.4%/ top only 2.2%**

The segregation is in fact a result of the motion of the liquid enriched with solute during solidification and of the purer liquid formed by melting the separated phases during melting part of the cycle.



# 10) Divorced eutectic

- The primary phase continues to solidify past the eutectic point (along the line EA) of Fig. 6.31 until either the whole of the liquid has solidified or the other phase nucleated and forms a layer, which is some times dendritic, separating the two layers of the primary phase.

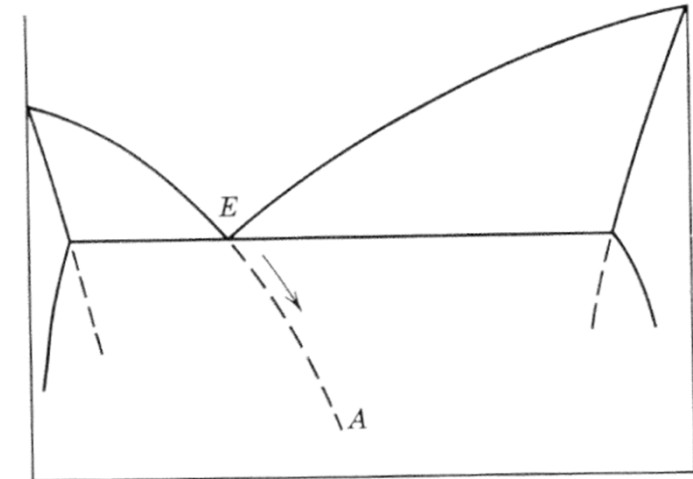
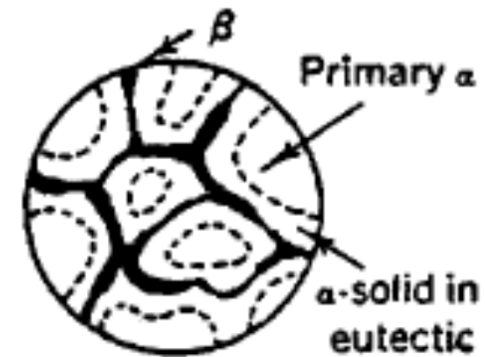


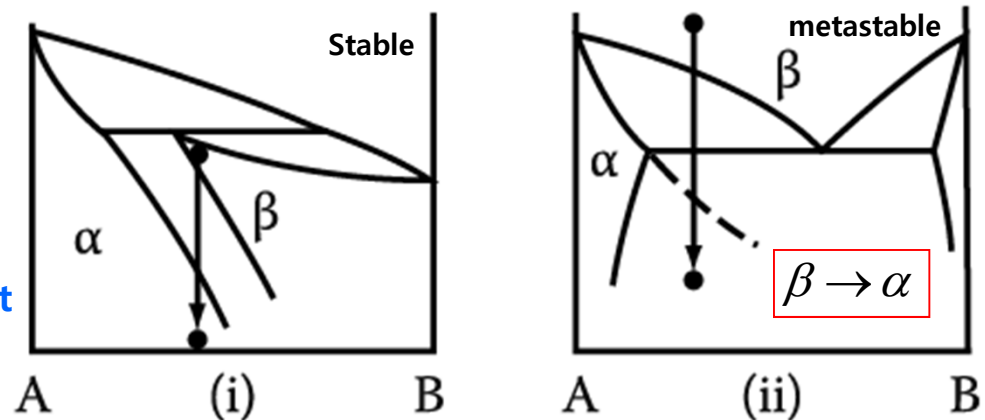
Fig. 6.31. Supercooling of eutectic in the absence of the second phase.

- One of the phases requires considerable supercooling for nucleation.
- “Divorced eutectic” is used to denote eutectic structures in which one phase is either absent or present in massive form.



## Massive Transformation

: The original phase decomposes into one or more new phases which have the same composition as the parent phase, but different crystal structures.



## 11) Ternary eutectic: very little work has been reported

\* lamellar form, alternating three phases in ternary eutectic of Pb-Sn-Cd

**: This arrangement is the one which would provide the shortest possible diffusion path for a given total area of interphase boundary, since each phase is adjacent to both of the other two phases.**

- IH \_ Summary of recently reported paper for Quar-ternary or higher eutectic (within 3 pages of PPT)

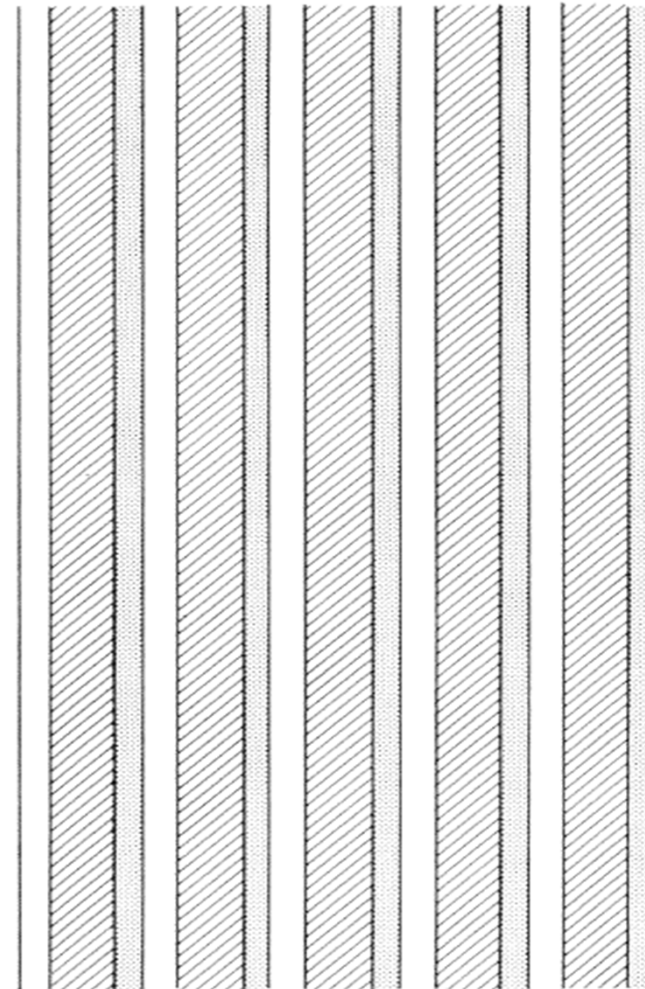


Fig. 6.34. Lamellar ternary eutectic.